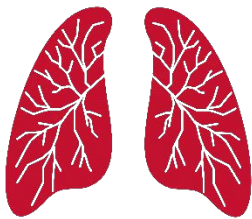


# Meakins-Christie Laboratories 50th Anniversary Symposium and Respiratory Research Day

## ABSTRACT BOOK



MEAKINS  
CHRISTIE



Centre universitaire  
de santé McGill  
Institut de recherche



McGill University  
Health Centre  
Research Institute



McGill

**Wednesday, May 17 – Thursday, May 18, 2023**

InterContinental Hotel, Old Montreal  
360 Saint-Antoine St. West, QC, H2Y 3X4  
Room: Sarah Bernhardt

## Day 2, Poster 24 - Effect of Long-acting Levodopa on Obstructive Sleep Apnea in Parkinson's Disease (ELO-PD trial): Preliminary Results

Amanda Scanga<sup>1,2</sup>, Andrea Benedetti<sup>2,3</sup>, Anne-Louise Lafontaine<sup>4</sup>, John R Kimoff<sup>5</sup>, Marianne Gingras<sup>5</sup>, Marta Kaminska<sup>1,2,5</sup>

<sup>1</sup>Division of Experimental Medicine, McGill University, Montréal, QC, <sup>2</sup>Respiratory Epidemiology and Clinical Research Unit, McGill University Health Centre, Montréal, QC, <sup>3</sup>Department of Epidemiology, Biostatistics and Occupational Health, McGill University, Montréal, QC, <sup>4</sup>Montréal Neurological Institute-Hospital, McGill University Health Centre, McGill University, Montréal, QC, <sup>5</sup>Respiratory Division, Sleep Laboratory, McGill University Health Centre, McGill University, Montréal, QC

**Background:** Obstructive sleep apnea (OSA) is common in Parkinson's disease (PD) and can lead to daytime sleepiness and cognitive dysfunction. Continuous positive airway pressure (CPAP) therapy is an effective treatment for OSA, however, adherence can be difficult for certain patients. Previous work showed that patients with PD taking long-acting levodopa (LALD) at bedtime had fewer respiratory disturbances during sleep. Thus, we hypothesize that, in PD patients with OSA, LALD taken at bedtime may reduce OSA severity, as measured by the apnea-hypopnea index (AHI).

**Methods:** In this pilot trial, 36 patients were randomized and allocated to either: group A - LALD followed by placebo (n=16) or group B - placebo followed by LALD (n=20). Treatment was administered daily at bedtime for two weeks, separated by a two-week washout period. The AHI was determined by polysomnography at screening, at the end of each treatment period, and at the end of the washout period (baseline 2). The change in AHI from baseline to intervention on LALD versus on placebo was assessed using a linear mixed model. A paired t-test was performed as a sensitivity analysis to compare the change in AHI from baseline on placebo and on LALD.

**Results:** The average age of our cohort was 65.6 years, with 80.5% of participants male and average body mass index of 27.9 kg/m<sup>2</sup>. The average PD duration was 4.7 years and the average baseline AHI was 30.7 events/hour. From the mixed model, the unadjusted difference in the change in AHI from baseline to LALD versus from the other baseline to placebo was 3.2 events/hour (95% confidence interval: -2.5; 8.9, p-value: 0.28). Including period or carryover effects did not substantially change results. By t-test, the mean difference in AHI on placebo versus on LALD was 2.1 (p-value = 0.65) for the total sample.

**Conclusion:** LALD does not seem to reduce OSA severity in this cohort overall. Next steps include exploring the clinical characteristics of participants who responded to the treatment versus those who did not.

# Day 1, Poster 4 & Oral Day 1 - Racial Disparities in Lung Biopsies for Interstitial Lung Diseases in Canada

Amanda Marino<sup>1</sup>, Jolene H Fisher<sup>2</sup>, Kerri A. Johnson<sup>3</sup>, Nasreen Khalil<sup>4</sup>, Martin Kolb<sup>5</sup>, Helena Manganas<sup>6</sup>, Veronica Marcoux<sup>7</sup>, Christopher J Ryerson<sup>4</sup>, Deborah Assayag<sup>1,8</sup>

<sup>1</sup>McGill University, <sup>2</sup>University of Toronto, <sup>3</sup>University of Calgary, <sup>4</sup>University of British Columbia, <sup>5</sup>McMaster University, <sup>6</sup>Université de Montréal, <sup>7</sup>University of Saskatchewan, <sup>8</sup>Respiratory Epidemiology and Clinical Research Unit (RECRU)

## Background

Surgical lung biopsies (SLB) remain an important step in the diagnosis and classification of interstitial lung diseases (ILD), especially when clinical and radiologic domains are non-diagnostic or conflicting. Sex and racial disparities exist in the care of patients with ILD. Although many studies have looked at indications for SLB, none to our knowledge have assessed sex and racial-based differences in undergoing a SLB in ILD. The objective of this study was to determine if patient sex assigned at birth or race influence having undergone a SLB for ILD.

## Methods

Using the CANadian REgistry for Pulmonary Fibrosis (CARE-PF), a multicenter, prospective registry of ILD patients, we performed this retrospective, observational study. Descriptive statistics were used to describe the population. Logistic regression was used to determine the baseline variables associated with having undergone SLB, with race (dichotomized as White and non-White) and sex as key independent variables. Multivariate analysis was performed to adjust for pre-determined confounders, including diagnostic subtype, age, forced vital capacity and diffusion of the lung for carbon monoxide. Time from initial clinic visit to SLB was assessed using Kaplan-Meier curve (log rank test).

## Results

Of the 4806 patients included in this study, 846 (18%) underwent SLB. Of those, 447 (53%) were male and 399 (47%) were female, and 695 (82%) are White (18% non-White). There was no significant difference in odds of undergoing SLB between men and women. However, patients of White race had 2.4 times the odds of undergoing SLB compared to those of non-White race (OR 2.4, 95% CI 1.76 to 3.29). When adjusting for diagnostic subtype, age, and physiology measures, this association remained significant (OR 1.81, 95% CI 1.27 to 2.58). Patients of White race were also significantly more likely to receive a biopsy earlier compared to those of non-White race (Figure 1,  $p < 0.001$ ).

## Conclusions

In this Canadian prospective cohort of ILD patients, those of White racial background have significantly higher odds of undergoing SLB compared to those of non-White ethnicity, after adjusting for diagnosis, age, and disease severity. Clinicians should be mindful of these biases when determining if their patient would benefit from SLB.

## Day 2, Poster 3 - Investigating gut microbiota determinants of IL-17-producing gdT cells during early life

Bavanitha Thuraiajah<sup>1,2,3</sup>, Katie Olsen<sup>1</sup>, Ghislaine Fontes<sup>2,3</sup>, Cynthia Faubert<sup>2</sup>, Irah King<sup>1,2,3</sup>

<sup>1</sup>McGill University, <sup>2</sup>RI-MUHC, <sup>3</sup>Meakins-Christie Laboratories

Interleukin-17 producing gd (gd17) T cells are a thymically-imprinted subset of innate-like T cells implicated in host defense against infection at barrier sites but also pathological conditions such as colorectal cancer. Although gd17 T cells seed peripheral tissues during embryogenesis, the impact of early-life events, such as microbial colonization of the intestine, on the activation and function of these cells remains to be determined. Here we use diverse gnotobiotic approaches in mice to examine the impact of the gut microbiota on intestinal gd17 T cell dynamics across the lifespan. We demonstrate that colonic gd17 T cells exhibit spontaneous secretion of IL-17 and IL-22 just prior to weaning, a time point coinciding with significant intestinal growth and robust expansion of the commensal microbiota. Using germ-free mice, we establish that the gut microbiota is critical for this early-life response and that fetal-derived Vg6+ gd T cells are the primary source of these cytokines. Further, we show developmental activation of gd17 T cells selectively occurs within the colonic lamina propria, requires IL-1 receptor signals and subsides with age. However, this response is not age-dependent as colonization of germ-free mice with a diverse microbial community during adulthood recapitulates early-life gd17 T cell activation. Reconstitution experiments using the feces of mice from diverse vivariums indicate that microbial composition, not simply colonization per se, determines the magnitude of colonic gd17 T cell activation. Collectively, our results provide new insight into mechanisms regulating intestinal gd17 T cells and set the stage for identifying specific microbial signals that shape the long-term function of this important innate-like T cell subset.

# Day 2, Poster 15 - Major Peanut Allergens Ara h 1, Ara h 2 and Ara h 8 Are Degraded and Fragmented Following High-Pressure and Temperature Autoclaving

Casey G. Cohen<sup>1,2</sup>, Kurt Dejgaard<sup>3</sup>, Bertrand J. Jean-Claude<sup>1</sup>, Bruce D. Mazer<sup>1,2</sup>

<sup>1</sup>Division of Experimental Medicine, Research Institute of the McGill University Health Centre, Montreal, Quebec, Canada, <sup>2</sup>Meakins-Christie Laboratories, RI-MUHC, McGill University, <sup>3</sup>Department of Biochemistry, McGill University, Montreal, Quebec, Canada

**Background:** Peanut allergy is a growing global health concern and is the leading cause of fatal anaphylaxis. The effects of various thermal processing methods on peanut allergenicity have been evaluated in recent decades. However, the specific allergen composition and structure under each condition has yet to be confirmed.

**Methods:** Raw, roasted, and autoclaved peanuts were processed into protein extracts and samples were run via SDS PAGE . Given that multiple peanut allergens are in the size range of 16 to 18 kDa (i.e. Ara h 2, Ara h 8), band regions from 15 to 20 kDa were excised and proteins were digested in-gel with trypsin prior to LC-MSMS analysis.

**Results:** SDS PAGE showed clear, distinct bands for the raw or roasted samples, whereas the autoclaved extract displayed no distinct bands and a smear. Proteomics analyses revealed multiple major allergens, including Ara h 1, Ara h 2 and Ara h 8. Striking differences were observed in the total spectral count profiles of the autoclaved sample, in which considerably lower spectral counts corresponding to Ara h 2 and Ara h 8 were obtained when compared to raw or roasted. Interestingly, higher spectral counts corresponding to Ara h 1, a major peanut allergen (63 kDa), were detected in the autoclaved sample. This is likely due to the migration of fragments resulting from extensive Ara h 1 degradation throughout the autoclaving process.

**Conclusions:** High-pressure and temperature autoclaving results in the degradation and fragmentation of major peanut allergens and thus may be a viable method for reducing allergenicity.

# Day 2, Poster 6 - Incorporation of clinical factors to improve the diagnostic accuracy of artificial intelligence-based chest X-ray analysis for detecting pulmonary tuberculosis

Coralie Geric<sup>1, 2, 3</sup>, Gamuchirai Tavaziva<sup>1, 3</sup>, Marianne Breuninger<sup>4</sup>, Keertan Dheda<sup>5, 6</sup>, Ali Esmail<sup>5</sup>, Monde Muyoyeta<sup>7, 8</sup>, Klaus Reither<sup>9, 10</sup>, Aamir Khan<sup>11</sup>, Andrea Benedetti<sup>1, 12</sup>, Faiz Ahmad Khan<sup>1, 3, 13</sup>

<sup>1</sup>McGill International TB Centre, Research Institute of the McGill University Health Centre, Montreal, Canada, <sup>2</sup>Department of Medicine, McGill University, Montreal, Canada, <sup>3</sup>Respiratory Epidemiology and Clinical Research Unit, Centre for Outcomes Research and Evaluation, Research Institute of the McGill University Health Centre, Montreal, Canada, <sup>4</sup>Division of Infectious Diseases, Department I of Internal Medicine, University of Cologne, Cologne, Germany, <sup>5</sup>Centre for Lung Infection and Immunity Unit, Division of Pulmonology and UCT Lung Institute, University of Cape Town, Cape Town, South Africa, <sup>6</sup>Faculty of Infectious and Tropical Diseases, Department of Infection Biology, London School of Hygiene and Tropical Medicine, London, United Kingdom, <sup>7</sup>Zambart, Lusaka, Zambia, <sup>8</sup>Centre for Infectious Disease Research in Zambia, Lusaka, Zambia, <sup>9</sup>Swiss Tropical and Public Health Institute, Basel, Switzerland, <sup>10</sup>University of Basel, Basel, Switzerland, <sup>11</sup>IRD Global, Singapore, <sup>12</sup>Department of Medicine and Department of Epidemiology, Biostatistics & Occupational Health, McGill University, Montreal, Canada, <sup>13</sup>Department of Epidemiology, Biostatistics & Occupational Health, McGill University, Montreal, Canada

## BACKGROUND

Chest X-ray (CXR) analysis with computer-aided detection (CAD) produces continuous scores on a 100-point scale. Common practice involves selecting thresholds to classify CXR as compatible with tuberculosis or not; however, selecting appropriate thresholds is challenging. We hypothesized that using CAD scores in a multivariable model with clinical information would increase tuberculosis detection accuracy over CAD alone.

## METHODS

Individual patient data was used from three studies that consecutively enrolled individuals seeking care due to symptoms of tuberculosis, and evaluated CAD using nucleic acid amplification or culture as the reference test.

CXR were analyzed using two commercially-available software. Separately for each software, we used logistic regression to model tuberculosis status. Crude models included CAD scores as the predictor; adjusted models added clinical factors selected a priori (age, sex, HIV status, and prior tuberculosis).

To evaluate model performance, we assessed calibration and discrimination. We internally validated models using bootstrap resampling. We compared receiver operating characteristic curves for crude and adjusted models using DeLong's p-value. We classified CXR using prediction cut-offs that achieved pre-specified sensitivities and calculated the specificity, positive predictive value, and negative predictive value.

## RESULTS

566/3308 (17%) of participants had microbiologically-confirmed pulmonary tuberculosis. Those with tuberculosis were less likely to previously had tuberculosis (13.6% vs 22.9%,  $p < 0.001$ ), and more likely HIV-positive (24.4% vs 12.9%,  $p < 0.001$ ).

For both software, compared to CAD alone, predictive power improved for adjusted models (DeLong's  $p\text{-value} < 0.001$ ), and the specificity and positive predictive value increased for all held sensitivities.

## CONCLUSION

Models incorporating clinical factors improved the predictive ability of two CAD software.

## Day 1, Poster 10 - Helminth-induced reprogramming of the stem cell compartment inhibits type 2 immunity

Danielle Karo-Atar<sup>1</sup>, Tanvi Javkar<sup>2</sup>, Loick Joumier<sup>3</sup>, Ghislaine Fontes<sup>1</sup>, Gregory J. Fonseca<sup>4</sup>, Marc Parisien<sup>5</sup>, Luda Diatchenko<sup>5</sup>, Jakob von Moltke<sup>6</sup>, Mohan Malleshaiah<sup>3</sup>, Alex Gragorieff<sup>2</sup>, Irah L. King<sup>1</sup>

<sup>1</sup>Department of Microbiology and Immunology, Meakins-Christie Laboratories, Research Institute of McGill University Health Centre, Montreal, Quebec, Canada , <sup>2</sup>Department of Pathology, McGill University and Cancer Research Program, Research Institute of McGill University Health Centre, Montreal, Quebec, Canada , <sup>3</sup>Division of Systems Biology, Montreal Clinical Research Institute (IRCM), 110 Avenue Des Pins Ouest, Montreal, QC H2W 1R7, Canada, <sup>4</sup>McGill University Health Centre, Meakins-Christie Laboratories, Department of Medicine, Division of Quantitative Life Sciences, Montreal, Quebec, Canada, <sup>5</sup>Department of Human Genetics, Allen Edwards Centre for Pain Research, McGill University, Montreal, Quebec, Canada, <sup>6</sup>Department of Immunology, University of Washington, Seattle, Washington, USA

Enteric helminths form intimate physical connections with the intestinal epithelium, yet little is known about the ability of helminths to directly shape the fate of this barrier tissue. Here we show that infection of mice with *Heligmosomoides polygyrus bakeri* (*Hpb*) induces a regenerative fetal-like state in the intestinal stem cell compartment, marked by the emergence of *Clusterin*-expressing revival stem cells (revSCs) and coincident with adult parasite adherence to intestinal villi. Organoid-based studies using parasite-derived excretory/secretory products reveal that *Hpb*-mediated revSC generation occurs independent of host-derived immune signals and inhibits type 2 cytokine-driven differentiation of secretory lineages that promote worm expulsion. In-depth analysis revealed that helminth-secreted products induce an oxidative stress response, critical for fetal-reversion of the intestinal stem cell compartment and lineage-tracing studies confirm the presence of revSC-derived progeny along the villi of *Hpb*-colonized animals. By contrast, type 2 cytokines inhibit revSC development and the fetal gene program both *in-vitro* and *in-vivo*, while deletion of type 2 cytokine signaling *in-vivo* lead to an enhanced fetal host response, increased host susceptibility to infection and improved worm fitness. Collectively, our study reveals how a helminth parasite co-opts a tissue development program to counter type 2 immune-mediated expulsion and maintain chronic infection.

# Day 1, Poster 12 - Serological Assessment of Patients Undergoing Peanut Oral Immunotherapy: The Role of IgG4

Diana Toscano-Rivero<sup>1,2</sup>, Casey G. Cohen<sup>1</sup>, Wei Zhao<sup>1</sup>, Eisha A. Ahmed<sup>1</sup>, Danbing Ke<sup>3</sup>, Liane Beaudette<sup>3</sup>, Duncan Lejtenyi<sup>3</sup>, Julia Upton<sup>4</sup>, Thomas Eiwegger<sup>4</sup>, Moshe Ben-Shoshan<sup>3</sup>, Bruce D. Mazer<sup>1,2,3</sup>

<sup>1</sup>Research Institute of the McGill University Health Centre, <sup>2</sup>Meakins-Christie Laboratories, McGill University, <sup>3</sup>Division of Allergy and Clinical Immunology, Department of Pediatrics, Montreal Children's Hospital, <sup>4</sup>Division of Immunology and Allergy, Department of Pediatrics, Hospital for Sick Children

**Background:** Peanut oral immunotherapy (OIT) aims to increase the safety of individuals with peanut allergy by gradual exposure to small, measured amounts of peanuts. Many studies use a maintenance dose of 300mg to achieve clinical desensitization. OIT is limited by frequent dose-related adverse reactions, leading to participant withdrawals. Data on immunologic parameters associated with maintenance doses lower than 300mg are limited.

**Methods:** Twenty-nine peanut-allergic children aged 1 to 19 years were enrolled in a trial (**NCT03532360**) of low (30mg) or high-maintenance dose (300mg) peanut OIT. Patients were randomized to 300mg (N=16) or 30mg (N=13) groups. Blood was drawn at two timepoints: oral food challenge and post-escalation challenge. Serum samples were used for quantitative detection of total peanut-specific immunoglobulin (Ig) E and IgG4 levels by ELISA.

**Results:** After a median escalation phase of 16 months, peanut-specific-IgG4 significantly increased from a median baseline of 89.53µg/mL (IQR 30.03-189.32) to 453.19µg/mL (IQR 75.77-1466.71) in the 300mg group ( $p<0.001$ ) and from 184.29µg/mL (IQR 35.00-585.88) to 803.11µg/mL (IQR 237.12-953.60) in the 30mg group ( $p<0.01$ ). Peanut-specific-IgE did not significantly change over time in either group, from a median baseline of 117.60ng/mL (IQR 1.56-1401.31) to 699.76ng/mL (IQR 1.56-1528.86) in the 300mg group and from 93.38ng/mL (IQR 47.44-645) to 90.82ng/mL (IQR 23.6-912) in the 30mg group ( $p>0.05$ ). The IgG4/IgE ratio significantly increased over the course of peanut OIT in both groups ( $p<0.001$ ). There were no significant differences between groups for both peanut-specific-IgG4 and IgE levels in the post-escalation challenge. Finally, there was a significant association between the IgG4 levels and the eliciting dose at the oral food challenge with peanut OIT for both groups ( $p<0.01$ ).

**Conclusions:** Our findings suggest that both low- and high-maintenance doses do not differ in terms of the efficacy of the protocol, since both groups reached similar eliciting doses at the post-escalation challenge. Our results may improve the current peanut OIT regimens and allow for a reduction in the maintenance doses.



# Day 1, Poster 28 - Heterogeneous Regulation of IL-10 Expression in B-cell Subsets

Eisha Ahmed<sup>1,2</sup>, Nicholas Vonniessen<sup>1,2</sup>, Wei Zhao<sup>1,2</sup>, Bruce Mazer<sup>1,2</sup>

<sup>1</sup>Research Institute of the McGill University Health Centre, <sup>2</sup>Meakins-Christie Laboratories, McGill University

Regulatory B-cells (Bregs) are a heterogeneous cell subset of growing interest with the capacity to suppress inflammatory responses. The most studied class of Bregs are those defined by the expression of interleukin-10 (IL-10), however B-cell subsets which express IL-10 and their mechanism of IL-10 induction remains unclear. Toll-like receptor activation is known to induce IL-10 expression in both mouse and human B-cells, with CpG - a TLR9 agonist - commonly used to induce Bregs in vitro. In this study, we use CpG to induce and study IL-10 regulation across mouse B-cell subsets, identify signalling pathways crucial for IL-10 expression, and explore transcriptomic relationships between IL-10+ B-cells derived from multiple B-cell subsets. Using primary cells from IL-10-reporter mice, we have found that mouse B-cell subsets differ in their capacity to express IL-10 in response to CpG stimulation. Splenic marginal zone (40% IL-10+) and splenic B1 cells (50% IL-10+), and peritoneal B1 cells (70% IL-10+) exhibit the greatest IL-10 competence compared to follicular B (10% IL-10+) and peritoneal B2 (25% IL-10+) subsets after 48 hours. Peritoneal B-cells were capable of upregulating IL-10 expression more rapidly than splenic B-cells, and IL-10 induction in splenic B-cells was p38 dependent. Breg gene expression significantly differed based on the originating subset. Our results show that cell-intrinsic heterogeneity contributes to Breg heterogeneity in behaviour and phenotype, significantly influencing IL-10-competence. This work highlights the necessity of deconvoluting heterogeneous cell responses to better understand mechanisms of gene regulation due to the significant differences between lymphoid and circulating B-cell populations.

## Day 2, Poster 25 - The role of GATA6<sup>+</sup> peritoneal macrophages in host defense against influenza infection

Elizabeth Lapshina<sup>1,2</sup>, Erwan Pernet<sup>3</sup>, Maziar Divangahi<sup>1,2</sup>

<sup>1</sup>McGill University, <sup>2</sup>Meakins-Christie Laboratories, <sup>3</sup>University of Quebec - Trois-Rivieres

Influenza A virus (IAV) remains one of the most successful human pathogens, responsible for one of the most devastating pandemics in history and yearly epidemics to this day. Severe disease and death associated with influenza are often caused by a dysregulated host immune response, which causes massive lung damage leading to respiratory dysfunction. Therefore, suppressing the inflammatory immune response after viral clearance and promoting tissue repair is essential during influenza recovery. Most vertebrates have three major body cavities to protect and support internal organs: the pericardial, pleural and peritoneal cavity. During embryonic development, these cavities are seeded with tissue-resident macrophages, which are essential for cavity homeostasis and host defense against pathogens. In fact, the peritoneal cavity is protected by a dominating population of large tissue-resident macrophages that uniquely express a zinc-finger transcription factor, GATA6, that regulates their self-renewal, anatomical localization and survival. Recent evidence indicates that GATA6<sup>+</sup> large peritoneal macrophages (GLPMs) can mobilize to different sites of injury, such as the liver and intestines, to promote tissue repair. While previous work focused on models of sterile injury, there is limited literature examining how GLPMs respond in viral infections. Therefore, we aim to investigate how GLPMs migrate following IAV infection and their role in lung tissue repair. Insights into the cellular and molecular mechanisms of GLPMs will advance our understanding of their biological role in host defense against infections. Furthermore, delineating their repair potential may contribute to the development of new therapies against influenza viruses and other respiratory infectious diseases.

## Day 2, Poster 19 - AhR Controls Pulmonary Inflammation From Cannabis Smoke

Emily Wilson<sup>1,2</sup>, David Eidelman<sup>2,3</sup>, Carolyn Baglole<sup>1,2,3</sup>

<sup>1</sup>Department of Pharmacology and Therapeutics, <sup>2</sup>Meakins-Christie Laboratories, Research Institute of the McGill University Health Centre, McGill University, <sup>3</sup>Department of Medicine

$\Delta^9$ -Tetrahydrocannabinol (THC) is a well-known cannabinoid in *Cannabis sativa*. While THC may be anti-inflammatory, there is inconclusive literature on the effects of cannabis smoke on lung inflammation. This is relevant as inhaling cannabis smoke is the most common way that cannabis (marijuana) is consumed. Although cannabinoids classically interact with CB1 and CB2 receptors, non-G protein coupled receptors (GPCRs) can also interact with cannabinoids. This may include the aryl hydrocarbon receptor (AhR), a ligand-activated transcription factor highly expressed in the lungs that controls inflammation. We therefore hypothesize that the AhR is a key regulator of inflammation from cannabis smoke exposure.

To test this hypothesis, age-matched (8-12 weeks) heterozygous (*Ahr*<sup>+/-</sup>) and knock-out (*Ahr*<sup>-/-</sup>) mice were exposed to cannabis joints containing 0.5g dried cannabis (total THC: 200 mg/g; total CBD: <1 mg/g). Nose-only inhalation exposures were performed using SCIREQ® inExpose™ system twice per day in groups of two joints at 3 puffs/minute for 3 days. Plasma, bronchoalveolar lavage (BAL), and lungs were collected. THC ELISA was performed on the plasma. Cytokine profiling microarray was performed on plasma and BAL. Extracellular vesicles were extracted from the remaining BAL fluid. Proteins from lungs, extracellular vesicles (EVs), and cell-free BAL fluid were assessed through LC-MS/MS. Immune cells of the lung were assessed by flow cytometry.

Cannabis smoke activated the AhR only in *Ahr*<sup>+/-</sup> mice as indicated by increased *CYP1A1* mRNA expression in the lungs. Cannabis smoke exposed *Ahr*<sup>-/-</sup> mice had a decrease in percent viable cells as well as percentage of total immune cells in the lungs. AhR expression repressed cannabis-smoke induced increase in lung neutrophils. Total macrophages and monocyte populations remained unchanged; however, the monocyte populations shifted towards the inflammatory sub-type with an increase in Ly6C<sup>hi</sup> monocytes and a decrease in the Ly6C<sup>low</sup> monocytes. Lung compartments (tissue, EVs, and BAL fluid) show distinct protein profiles as well as inflammatory pathway enrichment from cannabis smoke treatments.

Acute cannabis smoke exposure activates the AhR and increases lung inflammation in the absence of AhR expression. Overall, this work investigates the consequences of cannabis smoke on lung inflammation and its therapeutic potential in lung health, pointing toward a pivotal role for the AhR.

## Day 2, Poster 8 - Production of antimicrobials in Canadian High Arctic Bacteria

Eszter Farkas<sup>1, 2</sup>, Evan Marcolefes<sup>3</sup>, Tiffany Leung<sup>1</sup>, Sanjay Cleveland Campbell<sup>4</sup>, Mina Nekouei<sup>4</sup>, Karine Auclair<sup>4</sup>, Lyle Whyte<sup>3</sup>, Samantha Gruenheid<sup>1</sup>, Dao Nguyen<sup>2, 5</sup>

<sup>1</sup>Department of Microbiology and Immunology, McGill University, Montreal, Canada, <sup>2</sup>Meakins-Christie Laboratories, Research Institute of the McGill University Health Centre, McGill University, <sup>3</sup>Department of Natural Resources Sciences, McGill University, Montreal, Canada, <sup>4</sup>Department of Chemistry, McGill University, Montreal, Canada, <sup>5</sup>Department of Medicine, McGill University, Montreal, Canada

New and effective antimicrobials are required to combat the current antimicrobial resistance crisis. Most clinical antimicrobials are derived from natural compounds produced by microbes to fight competing organisms in their environment. With a dry pipeline for antimicrobial development, researchers are exploring new avenues for identifying novel compounds. We propose to investigate bacterial isolates from the Canadian High Arctic, an extreme environment with high microbial diversity and unique environmental pressures. These characteristics contribute to the potential to select for bacteria that produce unique secondary metabolites. The goal of this project is to determine if Arctic isolates produce unique compounds with antibiotic applications. Screening of Arctic isolates from our collaborators in the Whyte lab led to the identification of five bacterial strains with antibacterial activity against several clinically relevant pathogens. We then characterized the antibacterial activity of organic extracts from these isolates against relevant clinical pathogens after confirming activity against the hyper-permeable and efflux deficient *E. coli*  $\Delta bamB \Delta tolC$ . One candidate extract was identified as having activity against multiple pathogens. We then developed a high-throughput bioluminescence assay to identify antimicrobial activity and used this assay to optimize antimicrobial production of our candidate isolate. We will use High-Performance Liquid Chromatography coupled to Mass Spectrometry to purify and identify the bioactive antibacterial compound(s). The structure of antibacterial compound(s) will then be elucidated using Nuclear Magnetic Resonance. This work will highlight the value of the Arctic bacterial isolates as a source for novel antimicrobials.

# Day 2, Poster 1 - Impact of Low Educational Attainment on Loss to Follow-up among Individuals Eligible for Lung Cancer Screening in a Quebec Pilot Lung Cancer Screening Program

Everglad Mugutso<sup>1,2</sup>, Charlotte Besson<sup>1</sup>, Rola Hamed<sup>3</sup>, Francine Noel<sup>1</sup>, Jana Taylor<sup>4</sup>, Anne Gonzalez<sup>1,5</sup>, Nicole Ezer<sup>1,2,5</sup>

<sup>1</sup>Centre for Outcomes Research and Evaluation, RI-MUHC, Montreal, QC, <sup>2</sup>Department of Experimental Medicine, McGill University, Montreal, QC, <sup>3</sup>Research Institute of the McGill University Health Centre, Montreal, QC, <sup>4</sup>Department of Diagnostic Radiology, McGill University, Montreal, QC, <sup>5</sup>Department of Medicine, McGill University, Montreal, QC

**Background:** Lung cancer screening using low-dose CT scan (LDCT) reduces lung cancer mortality by up to 20%. Most people who are eligible are not participating. Low educational attainment has been found to be a barrier to participation in other primary prevention programs.

**Methods:** The McGill University Health Centre (MUHC) lung cancer screening pilot program enrolled patients between January 2018 to June 2021. Lung cancer risk assessment was done using the PLCOm2012 calculator. Eligible patients had a PLCOm2012 score above 2%. Our study objective was to identify whether loss to follow-up (LTFU) was associated with low education and define whether this was mediated by low health literacy rates. Our primary outcome was LTFU, defined as not receiving a scheduled CT scan despite being eligible and without having withdrawn one's consent after a shared decision-making discussion. Covariates of interest were age, gender, level of education, smoking status, and presence or absence of COPD. Health literacy was defined by the 3-question validated health literacy screen (<3/5, defining low health literacy). Low education was defined as a high school education level or less. We performed multivariate logistic regression for data analysis.

**Results:** Among 230 patients assessed, 175 (76%) were eligible for lung cancer screening. Among those screened (n=112) median age was 64 years (IQR:6.25), 60(53%) had low educational attainment, 63 (60%) were current smokers, and 67 (60%) had self-reported COPD. Mean PLCOm2012 score was similar (LTFU group 5.76% (sd 3.71) versus no LTFU group 5.32% (sd3.74), p =0.43). In the subgroup who had health literacy assessed (n=99), 24 (24.3%) had inadequate health literacy. As expected, inadequate health literacy was higher in those with low educational attainment (p = 0.01). Among eligible individuals who had low educational attainment, LTFU was twice as likely compared to those with a high educational level. (OR 2.19 (95% CI: 1.07-4.64) after adjustment.

**Discussion:** Low educational attainment is a significant contributor of LTFU in lung cancer screening; health literacy mediates this relationship.

# Day 1, Poster 30 - Oscillometry and Spirometry in Fibrotic versus Non-Fibrotic Interstitial Lung Disease

Fanny Gabrysz-Forget<sup>1</sup>, Osmin AM Duran<sup>2</sup>, Ilan Azuelos<sup>1</sup>, Maxime Cormier<sup>1</sup>, Zoltan Hantos<sup>3</sup>, Ronald J Dandurand<sup>1, 2, 4</sup>, Deborah Assayag<sup>1, 2</sup>

<sup>1</sup>Department of Medicine, McGill University, <sup>2</sup>Research Institute McGill University Health Center, <sup>3</sup>Department of Anesthesiology and Intensive Therapy, Semmelweis University, Budapest, Hungary, <sup>4</sup>Lakeshore General Hospital, Pointe-Claire

## Rationale:

Patients with interstitial lung disease (ILD) can have difficulty performing traditional lung function tests due to the severity of their disease. Alternate methods to measure lung function should be considered. Oscillometry (Osc) is an effort-independent test using normal tidal breathing, measuring respiratory resistance (R) and reactance (X). This study aims to evaluate the correlation between spirometry, diffusion capacity of the lung for carbon monoxide ( $D_{LCO}$ ), and Osc in patients with fibrotic vs non-fibrotic ILD.

## Methods:

A cross-sectional study was conducted at the McGill University Health Center (Montreal, Canada). Osc was performed on the same visit as spirometry and  $D_{LCO}$ , using the tremoFlo® (Thorasys, Montreal, Canada). CT scans of the chest were reviewed for the presence of fibrotic or non-fibrotic ILD. Osc measures included resistance at 5 Hz ( $R_5$ , total respiratory system resistance) and at 5 minus 20 Hz ( $R_{5-20}$ , sensitive for small airway disease), reactance at 5 Hz ( $X_5$ , representing tissue elasticity), and reactance area (AX, reflecting the elastic properties of the lung and correlates with resistance measured at low frequencies). Osc parameters were compared to conventional physiology measures using Spearman's rho.

## Results:

Fifty-one patients were enrolled, with a mean age of  $65 \pm 14$  years. Patients had diagnoses of fibrotic ILD ( $n=30$ , 58%) and non-fibrotic ILD ( $n=21$ , 42%). Mean forced expiratory volume in one sec ( $FEV_1$ ) was  $2.10 \pm 0.75$  L, forced vital capacity (FVC) was  $2.70 \pm 0.98$  L,  $D_{LCO}$  was  $11.69 \pm 4.74$  ml/min/mmHg. Mean Osc results were  $R_5$ :  $4.05 \pm 1.60$  cmH<sub>2</sub>O/L/s,  $R_{5-20}$ :  $0.65 \pm 0.67$  cmH<sub>2</sub>O/L/s,  $X_5$ :  $-2.24 \pm 1.12$  cmH<sub>2</sub>O/L/s and AX:  $17.3 \pm 15.8$  cmH<sub>2</sub>O/L. In both fibrotic and non-fibrotic ILD, significant positive correlations were found between  $FEV_1$ , FVC and  $X_5$ , and significant negative correlations were found between  $FEV_1$ , FVC and AX. (Figure 1) Thus, respectively, showing that higher forced volumes correlate with greater lung elasticity, and with lower lung resistance. FVC did not significantly correlate with  $R_5$  nor  $R_{5-20}$ , in the presence or absence of fibrosis.  $D_{LCO}$  did not significantly correlate with the Osc measures.

## Conclusions:

In both fibrotic and non-fibrotic ILD,  $FEV_1$  and FVC correlate with the reactance Osc parameters, but not with the Osc resistance measures. Further studies need to be conducted to evaluate if Osc could eventually represent an easier alternative to traditional lung function tests for evaluating disease severity in ILD by measuring lung reactance.

**Financial support:** This work was supported by an investigator-initiated grant from Boehringer-Ingelheim Canada

# Day 1, Poster 21 - House Dust Mite-Induced Murine Model of Epicutaneous Allergic Inflammation and Atopic March

Fatima Hubaishi<sup>1</sup>, Rami Karkout<sup>1</sup>, Lydia Labrie<sup>1</sup>, Haya Aldossary<sup>1</sup>, Annie Beauchamp<sup>2</sup>, Jichuan Shan<sup>1</sup>, Louisr Cyr<sup>2</sup>, Brian J. Ward<sup>2</sup>, Elizabeth D. Fixman<sup>1</sup>

<sup>1</sup>Meakins-Christie Laboratories, Translational Research in Respiratory Diseases, RI-MUHC, McGill University,

<sup>2</sup>Research Institute of the McGill University Health Centre

**Background:** Early manifestation of atopic dermatitis (AD) in infants is associated with a higher risk of developing other allergic diseases (atopy) such as food allergy, rhinitis, and asthma. This progression is known as atopic or allergic march (AM) (Dharmage, et al. 2014). Here we present a detailed analysis of our recently developed acute Th2-skewed AD to AM model using clinically relevant allergen, house dust mite (HDM).

**Methods:** Female Balb/c mice were sensitized topically with HDM extract after mechanical disruption of the skin over the course of two weeks to induce AD-like skin inflammation. To examine AM to the lung, mice were challenged with HDM intranasally three weeks later to assess inflammatory responses to HDM in the lung.

**Results:** Mice sensitized with HDM in the skin showed a significant increase in dermal thickness, by histological analysis. Increased inflammation was confirmed by flow cytometry, where the frequency of CD45+ leukocytes (myeloid cells and CD4+ T cells) was increased in HDM- sensitized mice compared to control. An increase in the lung inflammatory response (eosinophils, Th2 CD4+ T cells, and Type 2 cytokines) was induced upon HDM challenge in mice that had been sensitized to HDM epicutaneously, compared to mice that been sensitized at either single site (skin or lung). This was accompanied by an increase in total serum IgE in the mice treated with HDM at both sites.

**Conclusions:** Based on a recent call for criteria for murine models relevant to human AD (Gilhar, et al. 2021), our model satisfies most of the criteria, compared to other studies in the literature. We present both innate inflammation and T cell adaptive immunity in AD and AM models using a clinically relevant allergen (HDM) with no added adjuvants or chemical irritants. We believe that our model will provide insight into the mechanism(s) driving AM from the skin to the lung.

# Day 1, Poster 13 - Effect of induced metabolic acidosis on the ventilatory and perceptual response to incremental cycle exercise testing in healthy adults

Felix Michel Girard<sup>1</sup>, Dennis Jensen<sup>1,2</sup>

<sup>1</sup>Clinical Exercise and Respiratory Physiology Laboratory, Department of Kinesiology and Physical Education, McGill University, Montreal, QC, Canada, <sup>2</sup>Research Institute of the McGill University Health Centre (RI-MUHC), Translational Research in Respiratory Diseases Program, Montreal, QC, Canada

**PURPOSE:** Examine the effects of induced metabolic acidosis on exertional breathlessness in healthy adults.

**METHODS:** In a randomized, single-blind, placebo-controlled, cross-over study, 12 healthy volunteers (31±3 yrs, mean±SEM; 3 men) performed symptom-limited incremental cardiopulmonary cycle exercise tests after ingesting 0.2 g of ammonium chloride (NH<sub>4</sub>Cl)/kg/day or 0.025 g sodium chloride (NaCl)/kg/day for 3 days. **RESULTS:** Compared with NaCl, NH<sub>4</sub>Cl induced a partially compensated metabolic acidosis: arterialized capillary [H<sup>+</sup>] increased by 12.5±2.0 nEq/L, while arterialized capillary PCO<sub>2</sub> and the plasma [strong ion difference] decreased by 8.0±1.7 mmHg and 9.1±1.2 mEq/L, respectively (all p£0.001). Exercise performance decreased after treatment with NH<sub>4</sub>Cl vs. NaCl: peak V·O<sub>2</sub>, peak power output and the duration of loaded pedaling decreased by 10%, 14% and 13%, respectively (all p£0.01). Compared with NaCl, NH<sub>4</sub>Cl increased the ventilatory response to exercise: ventilation (V·<sub>E</sub>), tidal volume (V<sub>T</sub>) and V·<sub>E</sub>/V·CO<sub>2</sub> increased by ~20%, 11% and 26%, respectively, with attendant reductions in end-tidal PCO<sub>2</sub> (by ~25%) at a standardized submaximal power output (iso-work) of 146 watts (all p£0.01). The magnitude of increased V·<sub>E</sub>/V·CO<sub>2</sub> at iso-work after treatment with NH<sub>4</sub>Cl vs. NaCl correlated with concurrent changes in [H<sup>+</sup>] at rest (r<sup>2</sup>=0.746, p<0.001). Breathlessness intensity ratings were significantly higher during exercise after treatment with NH<sub>4</sub>Cl vs. NaCl (by 1.1±0.3 Borg units at iso-work, p<0.01); however, breathlessness-V·<sub>E</sub> relationships were relatively preserved throughout much of exercise in NH<sub>4</sub>Cl vs. NaCl. Critical inspiratory constraints with attendant increases in breathlessness intensity ratings were observed near the limits of tolerance after treatment with NH<sub>4</sub>Cl vs. NaCl.

**CONCLUSIONS:** In conclusion, NH<sub>4</sub>Cl-induced increases in exertional breathlessness reflected the awareness of increased V·<sub>E</sub>, secondary to alterations in the regulated level of [H<sup>+</sup>]; and (2) critical inspiratory constraints contributed to breathlessness near end-exercise after treatment with NH<sub>4</sub>Cl. The results of this study provide insight into the mechanism(s) of exertional breathlessness among people with acute or chronic acid-base disturbances.



## **Day 1, Poster 6 - Proteomic changes induced by the stringent response that led to envelope adaptation and antibiotic tolerance in stationary phase *Pseudomonas aeruginosa***

Jacquelyn Rich<sup>1</sup>, Geoffrey McKay<sup>2</sup>, Annie Shao<sup>3</sup>, Chris Thibodeaux<sup>3</sup>, Dao Nguyen<sup>1, 2</sup>

<sup>1</sup>Department of Microbiology and Immunology, McGill University, Montreal, QC, Canada, <sup>2</sup>Meakins-Christie Laboratories, Research Institute of the McGill University Health Centre, Montreal, QC, Canada, <sup>3</sup>Department of Chemistry, McGill University, Montreal, QC, Canada

*Pseudomonas aeruginosa* (*Pa*) is an opportunistic pathogen known for causing recalcitrant chronic infections, such as in the lungs of those with cystic fibrosis. Antibiotic tolerance, the inducible ability of a bacteria to survive high concentrations of antibiotics even in the absence of resistance genes, has been observed in *Pa* during stationary phase, as well as in response to stress. Environmental stressors such as nutrient starvation, oxidative stress, or heat stress have all been shown to induce the stringent response (SR), through the accumulation of the small molecule (p)ppGpp, which shifts bacterial physiology away from active metabolic processes towards responding to the stress, consequently leading to antibiotic tolerance. In our lab, a (p)ppGpp-null mutant ( $\Delta$ SR) displays decreased virulence, increased cell envelope permeability and decreased survival against, and influx of, multiple classes of antibiotics. This suggests that the SR partially mediates survival against antibiotics by fortifying the cell envelope. Preliminary analysis using gas chromatography mass spectrometry (MS) confirmed that  $\Delta$ SR has considerable alterations to the composition of the membrane lipids, while liquid- chromatography MS has shown several proteins are differentially expressed in  $\Delta$ SR compared to WT. Proteomic analysis of the  $\Delta$ SR mutant showed higher expression of proteins involved in nutrient transport, lipopolysaccharide synthesis and several outer membrane porins. Higher expression of regulatory proteins and quorum sensing proteins were also observed. This research characterizes how the SR, which is induced by environmental stress, can lead to altered protein expression, cell wall adaptation and, consequently, survival against antibiotics.

## Day 2, Poster 2 - Real-Time Cytokine Profiling of Critically Ill Patients

Jana Abi-Rafeh<sup>1,2</sup>, Josie Campisi<sup>3</sup>, Raham Rahgoshai<sup>3</sup>, Nicholas Vonniessen<sup>1,2</sup>, Peter Goldberg<sup>3</sup>, Salman Qureshi<sup>1,2,3</sup>, Bruce Mazer<sup>1,2</sup>

<sup>1</sup>Translational Research in Respiratory Diseases Program, McGill University Health Centre Research Institute,

<sup>2</sup>Meakins-Christie Laboratories, McGill University, <sup>3</sup>Critical Care Program, McGill University Health Centre

Sepsis is a heterogeneous and dysregulated host response to infection. Though clinical recognition of sepsis and its treatment has improved over the years, the incidence and its associated morbidities in the aging population have been on the rise<sup>1,2</sup>. Currently, there is a large gap in understanding the fundamental mechanisms of sepsis pathophysiology and associated morbidities and mortality. Efforts to understand the immunological response of sepsis survivors compared to non-survivors, through the quantification of immune cell numbers and secreted cytokines in blood samples of patients have been largely unsuccessful. Functional analysis of the immune response during sepsis has potential to provide prognostic information and could also inform therapeutic decisions. The traditional Enzyme-Linked ImmunoSpot (ELISpot) assay measures the number and intensity of cytokine-secreting peripheral blood mononuclear cells. Recently, a novel whole blood ELISpot assay with excellent dynamic range and rapid turnaround time was used to immunophenotype patients with sepsis<sup>3</sup>. We hypothesize that this whole blood ELISpot assay will identify and discriminate septic patients from critically ill non-septic patients (CINS) and that septic patients with impaired levels of TNF- $\alpha$  and IFN- $\gamma$  may be prone to greater adverse outcomes and immune dysfunction, which can exacerbate sepsis-associated morbidities.

We will test this hypothesis in a prospective cohort study that will enroll 50 septic, 30 CINS patients and 30 healthy controls. Serial blood sample collection for the septic and CINS patients will take place on days 1, 4, 7( $\pm$ 1), 14( $\pm$ 2), 21( $\pm$ 2), and 28( $\pm$ 2) of the disease. A whole blood ELISpot assay will be used to characterize innate and adaptive immune function by enumerating TNF- $\alpha$  and IFN- $\gamma$ -secreting cells, respectively. Detection and quantification of potentially rare cytokine-secreting cells by ELISpot will provide a highly sensitive measurement and dynamic view of the host immune response. TNF- $\alpha$  and IFN- $\gamma$  ELISpot assays are conducted under three different conditions: unstimulated, LPS or CD3/CD28, respectively, and PMA/ionomycin.

Patient recruitment is currently ongoing and preliminary findings suggest that septic patients that succumb have a profound and prolonged suppression of innate and adaptive immune response, as compared to survivors and CINS patients. Moreover, the preliminary findings also suggest a trend in cytokine production within healthy controls, which will be used to evaluate differences in cytokine production within septic and CINS patients. Specifically, control samples exhibit strong TNF- $\alpha$  production in unstimulated conditions with a rise in TNF- $\alpha$  after LPS stimulation. Conversely, unstimulated IFN- $\gamma$  production was minimal with a slight increase in production after CD3/CD28 and PMA/ionomycin stimulation.

By tracking the innate and adaptive immune function and correlating the results with clinical outcomes, this study will provide insight on a patient's cytokine profile as a marker of disease severity. In conclusion, our results will improve the current understanding of sepsis pathogenesis and could also lead to a more personalized and patient-centred approach to treatment in the future.

## Day 1, Poster 5 - MYTHO is a novel regulator of skeletal muscle autophagy, mass and integrity

Jean-Philippe Leduc-Gaudet<sup>1,2</sup>, Anais Franco-Romero<sup>2</sup>, Marina Cefis<sup>3</sup>, Alaa Moamer<sup>1</sup>, Felipe E. Broering<sup>1</sup>, Giulia Milan<sup>2</sup>, Roberta Sartori<sup>2</sup>, Tomer Jordi Chaffer<sup>1</sup>, Maude Dulac<sup>3</sup>, Vincent Marcangeli<sup>3</sup>, Dominique Mayaki<sup>1</sup>, Laurent Huck<sup>1</sup>, Anwar Shams<sup>4</sup>, José A Morais<sup>5</sup>, Elise Duchesne<sup>6</sup>, Hanns Lochmuller<sup>7</sup>, Marco Sandri<sup>2</sup>, Sabah NA Hussain<sup>1</sup>, Gilles Gouspillou<sup>3</sup>

<sup>1</sup>Meakins-Christie Laboratories, Translational Research in Respiratory Diseases Program, Research Institute of the McGill University Health Centre, Montréal, Québec, Canada., <sup>2</sup>Venetian Institute of Molecular Medicine, Padova, Italy, <sup>3</sup>Département des Sciences de l'activité physique, Faculté des Sciences, Université du Québec à Montréal, Montréal, Québec, Canada., <sup>4</sup>Department of Pharmacology, College of Medicine, Taif University, P.O.Box 11099, Taif 21944, Saudi Arabia., <sup>5</sup>Division of Geriatric Medicine, MUHC-Montreal General Hospital, McGill University, Montreal, Québec, Canada., <sup>6</sup>Département des sciences de la santé, Unité d'enseignement en physiothérapie, Université du Québec à Chicoutimi, 555, boulevard de l'Université, Chicoutimi, Québec, G7H 2B1, Canada. , <sup>7</sup>Children's Hospital of Eastern Ontario Research Institute, Ottawa, Ontario, Canada

The loss of skeletal muscle mass and function can have dramatic health consequences. Skeletal muscle weakness and atrophy are found in a wide range of clinical conditions, including cancer cachexia, starvation, sepsis, and aging. Autophagy, an essential catabolic process removing damaged cytosolic components, plays critical roles in the regulation of muscle mass, function and integrity. Accumulating evidence indicates that insufficient or excessive autophagy can contribute to the development of skeletal muscle atrophy. The molecular mechanisms regulating autophagy are complex and still partly understood. In the present study, we identified and characterized a novel FoxO-dependent gene, d230025d16rik which we named MYTHO (Macroautophagy and YouTH Optimizer), as a novel regulator of autophagy and skeletal muscle integrity *in vivo*. Mytho was significantly up regulated in various models of skeletal muscle atrophy. Short-term depletion of MYTHO attenuated muscle atrophy caused by fasting, denervation, cancer cachexia and sepsis, while MYTHO overexpression was sufficient to trigger muscle atrophy. MYTHO knockdown resulted in a progressive increase in muscle mass associated with a sustained activation of the mTORC1 signaling pathway. Prolonged MYTHO knockdown was associated with severe myopathic features, including impaired autophagy, muscle weakness, myofiber degeneration, and extensive ultrastructural defects, such as accumulation of autophagic vacuoles and tubular aggregates. Inhibition of the mTORC1 signaling pathway using rapamycin treatment attenuated the myopathic phenotype triggered by MYTHO knockdown. We conclude that MYTHO is a novel key regulator of muscle autophagy, mass and integrity.

# Day 2, Poster 11 - The Th17 inflammation axis as a potential mediator of persistent fatigue symptom in post-COVID-19 condition

Jérôme Bédard-Matteau<sup>1,2</sup>, Simon Rousseau<sup>1,2</sup>

<sup>1</sup>McGill University, RI-MUHC, <sup>2</sup>Meakins-Christie Laboratories

**Background and Rationale :** The Coronavirus disease also known as COVID-19 is a serious infectious disease attributable to SARS-CoV-2 viruses. The range of symptoms is extremely wide; patients can be asymptomatic or with mild symptoms. Oppositely, patients can become seriously ill and require medical interventions that can potentially result in death (WHO, 2020). SARS-CoV-2 manifests primarily with respiratory tract infection and flu-like symptoms. However, as research on the disease advances, COVID-19 is now being recognized as a multi-organ disease involving the nervous system. Indeed, several neurologic manifestations of varying severity are being reported in about 36 to 82% of hospitalized patients around the world (Graham et al., 2021). Notably, fatigue or chronic fatigue syndrome (CFS) accompanied with cognitive impairment (Graham et al., 2021). Many hospitalized patients report having symptoms persisting for weeks or months following the acute illness constituting a “long COVID” syndrome that greatly affect the patient’s cognition and quality of life. The immune response in COVID-19 involves increased expression of circulating cytokines, including interleukin 17 (IL-17), secreted by T Helper cell (Th17) (De Biasi et al., 2020). Interestingly, a single-nucleotide polymorphisms (SNP) in IL-17F has been linked to chronic fatigue syndrome (CFS) (Metzger et al., 2008). Our objective is to investigate IL-17F role in persistent fatigue, in long COVID-19.

**Hypothesis :** We hypothesize that a higher level of IL-17F will be observable in patient that reported fatigue in post-COVID-19 conditions.

**Aims and Methods:** The first aim is to investigate the impact of IL-17F on endothelial cells, one of their important cellular targets (Roussel et al., 2010) that may bridge the cardiovascular system to CNS (Julian Stewart, 2004; Furlan et al., 1998 ; Fisher et al., 2009 and Pongratz and Rainer, 2014). We will grow human endothelial cell *in vitro*, and expose them to IL-17F, to examine changes in the actin cytoskeleton structure caused by COVID-19- associated cytokines. The impact of IL-17F on endothelial cells will be examined using a combination of confocal microscopy and targeted transcriptomic. The second aim will be to use MAP kinase inhibitors to modulate the change in endothelial functions tested using adhesion assays, permeability assays and electrical resistance assays. The third aim will check whether TH17- derived cytokines are associated with persistent fatigue in COVID-19. We will access the transcriptomic and proteomic data made available on a longitudinal cohort of SARS-CoV-2 positive participant by the Biobanque Québécoise de la COVID-19 (BQC19). The goal will be to assess whether TH17-derived cytokines (IL17A, B, C, D, E and F) are predictive of persistent fatigue.

**Anticipated Results:** Endothelial cells exposed to IL-17F show an increase appearance of stress fibers as well as changes in their actin cytoskeleton. We expect to find a higher level of IL-17F in patient reporting fatigue. By building a viable *in vitro* model of endothelial cells, we expect to get a better understanding of changes in the actin cytoskeleton and try to modulate these perturbances using pharmacological interventions.

**Discussion:** COVID-19 is a very dynamic area of research. Little is still known about the mechanisms and pathologies. Getting a better understanding will allow us to identify potential therapeutic targets or therapies to improve the quality of life of these “long COVID” haulers.

**Funding:** This project is funded by the Canadian Lung Association.

# Day 2, Poster 16 - Enabling Single-cell Studies for Large-scale Disease Cohorts

Jingtao Wang<sup>1, 2</sup>, Jun Ding<sup>1, 2</sup>

<sup>1</sup>Meakins-Christie Laboratories, Research Institute of McGill Health Centre, Montreal, QC, Canada, <sup>2</sup>McGill University

**1 Background** Single-cell sequencing technologies provide much higher resolution measurement of individuals' cellular status than traditional bulk sequencing, which only measures the average transcription of a group of cells. Single-cell data provides unrivalled opportunities to understand the complex mechanisms underlying various complex diseases. To understand disease pathogenesis and find biomarkers and drug targets, cohort studies track a large group of people over time and study factors impacting their health. However, the prohibitive cost of single-cell data prevents its large-scale application in cohort studies. Acquiring single-cell level information at an affordable price will significantly facilitate various disease studies in Quebec. Myriad existing computational methods (e.g., CIBERSORTx, Bisque) tackle this issue by deconvoluting bulk data samples into cell type proportion vectors. However, these deconvolution methods do not fully solve the issue because their results are only at the cell type level. All single-cell level analyses cannot be performed with the deconvoluted cell type level expressions. For example, cell pseudo-time and cell-cell interactions have shown to be critical in varying diseases, and they require the single-cell level, not cell-type, measurements. Unfortunately, we still lack a computational method that reconstructs real single-cell level measurements from bulk sequencing data.

To provide affordable single-cell level measurement for cohort studies, we will develop an accurate in-silico pipeline (Cohort Single-cell Semi-profiler) to reconstruct single-cell measurements of target individuals based on the bulk measurements (of all) and single-cell profiles of "representative" individuals. The developed Semi-profiler will be tested on a cohort of 130 COVID-19/Control patients to demonstrate the accuracy of the semi-profiling task. Validation experiments and clinical practices will be conducted to examine the results. To our best knowledge, our method is one of the first that can reconstruct real single-cell level measurements that allow all downstream single-cell analytics, which will surely promote the application of single-cell in large-scale disease cohort studies.

**2 Methods** Given a patient cohort, our semi-profiling pipeline takes bulk data of all patients and budget for single-cell experiment as input, and it outputs single-cell data (either real or semi-profiled) for all. In this section we are going to introduce the key component of our semi-profiling pipeline - a VAE-GAN model tailored for single-cell data distribution learning, and then elaborate the three steps of the semi-profiling pipeline. Figure 1 shows the overall semi-profiling pipeline and the details are explained in the following sub-sections.

**2.1 VAE-GAN for Single-cell Distribution Learning** We first study techniques improving the distribution learning of single-cell data because this is the foundation of the semi-profiling model (the semi-profiling process is a modified distribution learning process). Existing methods, e.g. SCVI, uses Variational Autoencoder (VAE), for learning the distribution of single-cell data, which includes learning meaningful latent representation for cells and reconstructing single-cell data. However, such methods still suffer from poor reconstruction performance and the learned latent representations fail to reflect cell type difference (poor cell type clustering performance). We improve the performance by applying the following techniques: 1. Adding a discriminator typically used in a Generative Adversarial Network (GAN) to improve data reconstruction; 2. Using graph neural network (GNN) to incorporate similar cells' information when processing each cell; 3. Giving more importance to highly variable genes; 4. Improving data pre-processing. These techniques significantly improve the distribution learning. The Adjusted Rand Index (ARI) score of cell type clustering is improved from 0.71 to 0.83 compared to the version without these techniques.

**2.2 Semi-profiling Pipeline Step I - Select Initial Representatives** Our semi-profiling pipeline starts with selecting some representative patients for single-cell sequencing based on affordable bulk data. We represent parents

using their bulk gene expression data, reduce the feature dimension using Principal Component Analysis (PCA), cluster the reduced features using K-means, and select the patient closest to the cluster centroids as the representatives.

**2.3 Use VAE-GAN to Infer Single-cell Measurement of Target Patients according to Their Bulk Data and the Representatives' Single-cell Data** Panel (e) of figure 1 gives the architecture of our semi-profiling model. The VAE-GAN first learns to reconstruct the representative's single-cell data. Then we incorporate target patient's information by fine-tuning the model with a constraint: the average gene expression of the generated cells should be similar to the target bulk data. This constraint provides the model with bulk information of the target patient and guides the model to generate cells of the target patient.

**2.4 Select More Representatives using Active Learning to Improve Semi-profiling** If the budget allows, our active learning module can select more representatives for single-cell sequencing that helps the model best improve the semi-profiling performance. We compute the distance between patients based on their bulk gene expression difference and their single-cell (real or semi-profiled) gene expression difference. Then, since our hypothesis is that closer distance between the representative and the target patient will lead to better semi-profiling performance, we design an Expected Error Reduction Active Learning Algorithm for selecting the new representatives.

First, the patient cluster with the highest in-cluster heterogeneity (total distance from every patient to the representative) is selected. Then for each cluster member, compute the expected heterogeneity decrease if this patient is selected as new representative. The patient that can decrease the cluster heterogeneity the most will be selected as new representative.

Active learning-based representative selection and semi-profiling can be run iteratively to improve the performance until running out of budget. Active Learning can help cohort studies save costs by only sequencing the most informative patients.

**3 Results** Generally, on this 130 patient COVID-19 cohort, we propose that our semi-profiling pipeline can simulate single-cell data of high accuracy (good enough for single-cell level downstream analysis) with less than 20% cost.

Figure 2 shows the overall performance of two semi-profiling methods: a naïve semi-profiling method that always outputs patients' representatives' single-cell data; and our proposed semi-profiling method. Both methods get lower error (left y-axis) and higher cost (right y-axis) as more patients are sequenced (x-axis). But our semi-profiling method with active patient selection can get lower error given the same cost, or lower cost given the same error.

Additionally, we found sequencing 20 patients can already lead to very good semi-profiling, i.e. the simulated cells are very similar to the ground truth. This part of the results are shown in figure 1 Panel (g), (h) and (i) where we compare the downstream analysis results using real and semi-profiled data.

Figure 1 Panel (g) shows the UMAP visualization of the semi-profiled cells of the 130 patient cohort are nearly identical to the ground truth. Panel (h) shows the enrichment analysis results are the same using semi-profiled VS ground truth cell data. Panel (i) shows the cell type proportions of patients with different severity levels are almost the same between semi-profiled and ground truth. For cell type proportion estimation, we also evaluate our method as a cell type deconvolution method and compare with two state-of-the-art methods CIBERSORTx and Bisque. In terms of person correlation between ground truth and estimation, our method is similar or better than CIBERSORTx and significantly better than Bisque. These results demonstrate our semi-profiled cells are similar enough to the ground truth that they can be used for down-stream single-cell level analysis.

**4. Conclusions and Discussions** We developed single-cell semi-profiling pipeline based on deep generative learning model that can infer patient's single-cell data based on their bulk data and similar patient's single-cell

data. The semi-profiled data gives similar downstream analysis results as the original real data. Meanwhile, our semi-profiling method only requires the expensive single-cell data for only a few selected representatives, which largely reduces the cost, making it possible to using single-cell data for large-scale cohort study. Nevertheless, the semi-profiling performance is bad when the difference between representatives and target patients is large. In such case, more representatives should be selected to ensure each patient is “well represented”. In disease cohorts like cancer cohorts, patients have very different transcriptomic profile so that more representatives should be selected. Deciding how many representatives can be regarded as enough is an important future direction.

# Day 2 Oral- Residual respiratory disability after successful treatment of pulmonary tuberculosis: a systematic review and meta-analysis

Joshua Taylor<sup>1</sup>, Mayara Bastos<sup>1</sup>, Sophie Lachapelle-Chisolm<sup>1</sup>, Nancy Mayo<sup>2,3</sup>, James Johnston<sup>4</sup>, Dick Menzies<sup>1,2,3</sup>

<sup>1</sup>Respiratory Epidemiology and Clinical Research Unit, Research Institute of the McGill University Health Centre, Montreal, Canada, <sup>2</sup>Departments of Epidemiology, Biostatistics and Occupational Health, and Medicine, McGill University, Montreal, Canada, <sup>3</sup>Centre for Outcomes Research and Evaluation, McGill University, Montreal, Canada, <sup>4</sup>Department of Medicine, University of British Columbia, Vancouver, Canada

**BACKGROUND:** Pulmonary tuberculosis (PTB) can result in long-term health consequences, even after successful treatment. We conducted a systematic review and meta-analysis to estimate the occurrence of respiratory impairment, other disability states, and respiratory complications following successful PTB treatment.

**METHODS:** We identified studies from January 1, 1960, to December 6, 2022, describing populations of all ages that successfully completed treatment for active PTB and had been assessed for at least one of the outcomes of interest: occurrence of respiratory impairment, other disability states, and respiratory complications following PTB treatment. Studies were excluded if they reported on participants with self-reported TB, extra-pulmonary TB, inactive TB, latent TB, or if participants had been selected for having more advanced disease. Study characteristics and outcome-related data were abstracted. Meta-analysis was performed using a random effects model. We adapted the Newcastle Ottawa Scale to evaluate the methodological quality of the included studies. Heterogeneity was assessed using the  $I^2$  statistic and prediction intervals. This study is registered with PROSPERO (CRD42021276327).

**RESULTS:** 61 studies with 41,014 participants with PTB were included. In 42 studies reporting post-treatment lung function measurements, 59.1% ( $I^2=98.3\%$ ) of participants with PTB had abnormal spirometry compared to 5.4% ( $I^2=97.4\%$ ) of controls. Specifically, 17.8% ( $I^2=96.6\%$ ) had obstruction, 21.3% ( $I^2=95.4\%$ ) restriction, and 12.7% ( $I^2=93.2\%$ ) a mixed pattern. Among 13 studies with 3179 participants with PTB, 72.6% ( $I^2=92.8\%$ ) of participants with PTB had a Medical Research Council dyspnea score of 1-2 and 24.7% ( $I^2=92.2\%$ ) a score of 3-5. Mean six-minute walk distance in 13 studies was 440.5 metres ( $I^2=99.0\%$ ) in all participants (78.9% predicted,  $I^2=98.9\%$ ) and 403.0 metres ( $I^2=95.1\%$ ) among MDR-TB participants in 3 studies (70.5% predicted,  $I^2=97.6\%$ ). Four studies reported data on incidence of lung cancer, with an incidence rate ratio of 4.0 (95%CI 2.1-7.6) and incidence rate difference of 2.7 per 1000 person-years (95%CI 1.2-4.2) when compared to controls. Quality assessment indicated overall low-quality evidence in this field, and heterogeneity was high for pooled estimates of nearly all outcomes of interest.

**CONCLUSIONS:** The occurrence of post-PTB respiratory impairment, other disability states, and respiratory complications is high, adding to the potential benefits of disease prevention, and highlighting the need for optimized management after successful treatment.



## Day 2, Poster 4 - Maternal sleep-disordered breathing in pregnancy and risk of adverse health outcomes in mothers and children: Preliminary Results from a Pilot Study

Joshua Smocot<sup>1</sup>, Evelyn Constantin<sup>1</sup>, Nelly Huynh<sup>2</sup>, Frédéric Sériès<sup>3</sup>, Jean Séguin<sup>2</sup>, Isabelle Marc<sup>3</sup>, R John Kimoff<sup>1</sup>, William Fraser<sup>4</sup>, Andrea Benedetti<sup>1</sup>, Lorena Iglesias<sup>1</sup>, Osmin Duran<sup>1</sup>, Patricia Li<sup>1</sup>, Michael Zappitelli<sup>5</sup>, Tamara Cohen<sup>6</sup>, Sushmita Pamidi<sup>1</sup>

<sup>1</sup>McGill University, <sup>2</sup>Université de Montréal, <sup>3</sup>Université Laval, <sup>4</sup>Université de Sherbrooke, <sup>5</sup>University of Toronto, <sup>6</sup>University of British Columbia

**Rationale:** Sleep-disordered breathing (SDB) affects 17-45% of pregnant women and is associated with adverse health outcomes. However, it remains unclear whether exposure to maternal SDB during pregnancy adversely affects 1) health outcomes of offspring later in life and 2) indices of cardiometabolic health in mothers measured years after delivery. We are conducting a prospective cohort study which aims to address these important knowledge gaps. Here, we report preliminary results from the pilot phase of this study, which aims to determine the feasibility of performing key home-based measurements in mothers and children including ambulatory sleep studies, 24-hour ambulatory blood pressure monitoring (ABPM), actigraphy, anthropometric measurements and questionnaires.

**Methods:** Mother-child dyads (~8-11 years after delivery) are recruited from the 3D (Design, Develop, Discover) pregnancy birth cohort in Québec City and Montreal. During a single home visit (to minimize participant burden), sleep study installation, instruction for next-day 24-hour ABPM, 7-day actigraphy, anthropometric measurements and sleep questionnaires are completed for both mother and child. While a sample size of n=160 for the exposed group (SDB during pregnancy) and n=232 for the unexposed group (no SDB during pregnancy) is planned for the larger study, the pilot phase includes a total of 40 participants. To diagnose SDB, American Academy of Sleep Medicine (AASM) criteria were used in children (Level 2 home sleep apnea test) and mothers (Level 3 home sleep apnea test).

**Results:** Since March 2022, 13 mother-child dyads have been recruited with (mean±SD) maternal age 43.7±2.8 years and child age of 9.9±0.7 years. The mothers had a mean BMI of 25.6±5.7 kg/m<sup>2</sup> (5/13 (38.4%) were overweight or obese). All mothers completed sleep studies, having a mean AHI of 9.1±4.7 events/h and 3% ODI of 5.4±5.7 events/h. The oximeter signal for the maternal studies was reliable 97.0±6.9% of the time and the nasal cannula 100% of the time. For the children, BMI z-scores ranged from -0.82 to 2.0 (2/13 were at risk or were overweight). All children completed the sleep test. For the 5 sleep studies that have been scored to date, the mean AHI was 2.8±0.6 events/h, mean 3% ODI 1.1±0.4 events/h, and mean microarousal index 17.9±4.5 events/hour. The mean signal quality of the children's oximeter studies was 84.5±20.0% and the nasal cannula was 84.4±34.8%. 85% of mothers (n=11) completed the ABPM. While 85% of children also completed the ABPM, 6/11 (54.5%) had more than 70% valid measurements. Actigraphy was accepted by all participants (mother and child) and the mean recording duration was 7±1 days for both mothers and children.

**Conclusion:** The pilot phase of the follow-up study of the 3D Cohort reveals that home-based simultaneous sleep study and outcome measurements in mothers and children are feasible, minimizing participant burden but also ensuring adequate signal quality. The funded, larger cohort study will yield invaluable insight on long-term maternal and child health outcomes linked to maternal SDB in pregnancy.

**Research Funding Source:** Canadian Institutes of Health Research (CIHR; PJT 165975) and the Fonds de Recherche du Québec-Santé Réseau en Santé Respiratoire Team Grant

## Day 1, Poster 3 - Immunity to influenza A virus during pregnancy: An unexpected mechanism of resistance

Julia Chronopoulos<sup>1, 2</sup>, Erwan Pernet<sup>1, 2</sup>, Toby K. McGovern<sup>1, 2</sup>, Arina Morozan<sup>1, 2</sup>, Maziar Divangahi<sup>1, 2</sup>, James G. Martin<sup>1, 2</sup>

<sup>1</sup>Meakins-Christie Laboratories, McGill University, Montreal, Canada, <sup>2</sup>Research Institute of McGill University Health Centre, Montreal, Canada

Host survival during infection requires a delicate balance between host resistance, which is essential for eliminating pathogens, and disease tolerance, which is critical in minimizing tissue damage. Pregnant women represent a high-risk group during influenza A (IAV) outbreaks, in part due to type-2 immune responses which favor reproductive fitness. However, pregnancy in both humans and rodents induces a robust inflammatory response following IAV infection. Thus, it is still unclear how pregnancy regulates immunity to IAV and whether impairment in pulmonary antiviral immunity or an exorbitant inflammatory state contribute to maternal morbidity. We aimed to characterize both host resistance and disease tolerance in mid gestation C57BL/6 pregnant mice following IAV infection.

Wildtype non-pregnant and pregnant mice were intranasally infected with H1N1 (PR8; 50pfu). Unexpectedly our data indicated that pregnant mice were remarkably more resistant to IAV infection and were able to inhibit IAV replication within hours of infection. Due to this early control of viral replication, the magnitude of cellular immune responses, cytokines, and pulmonary immunopathology were significantly reduced. The increased disease tolerance in IAV-infected pregnant mice consequently preserved lung function. Interestingly, the drivers of maternal host defense to IAV appeared to be attributed to a broad enhancement of antimicrobial proteins in the nasal cavity and bypassing the upper airways via intratracheal infection abrogated protection.

Collectively, these findings indicate that pregnancy confers protection against IAV infection via enhancing host resistance in the nasal epithelium. Evolutionarily, pregnancy may alter the mode of host defense against pulmonary pathogens by augmenting upper airway antimicrobial immunity to minimize dissemination into the lower airways, limit lung tissue damage, and maintain optimal lung function to support maternal fitness.

# Day 1, Poster 7 - scCross: Single-cell multi-omics data intergration and cross-modal generation

Xiuhui Yang<sup>1</sup>, [Jun Ding](#)<sup>2</sup>

<sup>1</sup>Shangdong University, <sup>2</sup>Meakins-Christie Laboratories, Translational Research in Respiratory Diseases Program, RI-MUHC, McGill University

Single-cell multi-omics datasets hold great promise for understanding complex biological processes from a comprehensive perspective. However, the integration of different modalities poses a challenge due to their distinct feature spaces. Here we present scCross, an algorithm that uses a combination of variational autoencoder and generative adversarial network (VAE-GAN) to integrate features from different modalities and learn joint cell embeddings. We applied scCross to integrate and analyze various single-cell multi-omics data, including dual- and triple-omics data. scCross maps all modalities to a shared latent space, allowing for various downstream analytic tasks. It outperforms existing methods for data integration of single-cell multi-omics data and can generate single-cell data across modalities. Furthermore, scCross can infer intra- and inter-modal perturbations to manipulate cellular states, enabling the discovery of interventions and therapeutics against diseases. Our method provides a powerful tool for unlocking the potential of single-cell multi-omics data in advancing our understanding of complex biological processes.

# Day 1, Poster 11 - Understanding the roles of SHC4, FGFR signaling and NETosis in COVID-19 coagulopathy

Katelyn Liu<sup>1,2</sup>, William Ma<sup>3</sup>, Antoine Soulé<sup>3</sup>, Catherine Allard<sup>4</sup>, Salman Qureshi<sup>1,2</sup>, Karine Tremblay<sup>5</sup>, Amin Emad<sup>3</sup>, Simon Rousseau<sup>1,2</sup>

<sup>1</sup>Meakins-Christie Laboratories, Research Institute of the McGill University Health Centre, <sup>2</sup>Department of Medicine, Faculty of Medicine, McGill University, Montreal, QC, Canada, <sup>3</sup>Department of Electrical and Computer Engineering, McGill University, Montreal, QC, Canada, <sup>4</sup>Statistical Department, Centre de recherche du Centre hospitalier universitaire de Sherbrooke (CRCHUS), Sherbrooke, Canada, <sup>5</sup>Pharmacology-Physiology Department, Faculty of Medicine and Health Sciences, Université de Sherbrooke, Sherbrooke, Canada

**INTRODUCTION** Since the early stages of the pandemic, numerous studies from different countries report the presence of abnormal coagulation in severe COVID-19, as well as linking this manifestation to the organ injuries observed in the severe cases [1]. To this date, the pathogenesis of COVID-19 coagulopathy remains unclear. Studies link unbalanced neutrophil activities to severe COVID-19 and COVID-19 coagulopathy. Elevated levels of circulating neutrophils and markers of neutrophil extracellular traps (NETs) have been used as predictors for severe disease outcomes [3]. Moreover, NETs are observed in the presence of vascular thrombi in lung tissue samples from severe COVID-19 patients [3]. In a recent computational study conducted on data acquired in the Banque Québécoise de la COVID-19 (BQC-19), we have identified an endophenotype, EP6, that is associated with worst COVID-19 outcomes [2]. Patients in this subset are enriched in coagulopathy markers, as well as markers for NETs [2]. Pathway enrichment analysis on the aptamers associated with EP6 revealed that while EP6 is characterized by pathways associated with interleukins and cytokine signaling in the immune system, multiple instances linked it with FGFR signaling [2]. GWAS analysis on EP6 revealed that SHC4, an unwell characterized intracellular adaptor protein, may play an important mechanistic role in contributing to severe disease pathology [2]. The sum of these studies reveals roles for NETs, FGFR signaling, and SHC4 towards severe COVID-19 pathogenesis, namely in COVID-19 associated coagulopathy. However, little is understood about the interrelationship between these three entities in COVID-19, and more importantly little is understood about the pathogenesis of COVID-19 coagulopathy.

**HYPOTHESIS & AIMS** Taking the associations and evidence presented above together, I hypothesize that in the context of severe COVID-19, SHC4 is involved in FGFR signaling in neutrophils, promoting NET production, and thereby contributing to COVID-19 associated coagulopathy. I aim to determine 1) whether SHC4 is present in neutrophils or other immune cells, 2) whether FGFR signaling is involved the process of NET production, 3) whether differential expression of SHC4 affects NET production, and 4) whether key inflammatory mediators observed in COVID-19 (e.g., IL-6) affect SHC4 expression levels, FGFR signaling, and NET production.

**METHODS & RESULTS** SHC4 has not been found to be expressed in tissues outside the brain or the male reproductive organs previously. The data generated from the BQC-19 show an elevated level of SHC4 in circulation. In this current project, the first aim was to locate the source of the SHC4 signal. From western blot analysis, SHC4 has repeatedly been detected in HL-60 cells (a leukemia cell line), HL-60 differentiated into neutrophil-like cells, Beas-2B cells (lung epithelial cell line), and macrophage-like THP-1 cells. The findings were confirmed by flow cytometry assays as well, although the proportion of cells expressing SHC4 in the mentioned groups were near null except for HL-60 cells. The current target is to identify under which circumstances, SHC4 expression may be induced and upregulated. Given that primary human neutrophils have a short lifespan in blood circulation (estimated to be less than 24h), utilizing an immortalized cell line that can be differentiated into neutrophil-like cells is more suitable for in vitro studies. The human acute myeloid leukemia suspension cell line, HL-60, was used to derive the neutrophil model, as it can be differentiated towards a neutrophil-like phenotype using inducers such as DMSO, all-trans-retinoic acid (ATRA), and DMF. Differentiation yielded an increase in CD11b expression and nuclear lobularity. Subsequent treatment with phorbol 12-myristate 13-acetate yielded NETs after 4 hours of incubation. This in-vitro NETosis model will be used evaluate NETosis under various COVID-19 pathological conditions.

# Day 1, Poster 24 - The cross-protection of BCG vaccination in influenza infection: Training adaptive immunity?

Kim A. Tran<sup>1</sup>, Jun Ding<sup>1</sup>, Maziar Divangahi<sup>1</sup>

<sup>1</sup>Meakins-Christie Laboratories, Translational Research in Respiratory Diseases, RI-MUHC, McGill University

Influenza A virus (IAV) is the infectious cause for the most devastating pandemic in history and still bears considerable pandemic potential in the form of seasonal outbreaks and highly pathogenic avian influenzas (HPAI). Despite vaccination programs, circulating IAV strains are responsible for 250 000 to 500 000 deaths per annum while potential emergent strains are under constant surveillance by the WHO. The ongoing pandemic has especially highlighted the need for alternative approaches against the threat of emerging respiratory viruses such as SARS-CoV-2 and IAV. The Bacillus Calmette-Guerin (BCG) vaccine is used worldwide to prevent tuberculosis but has also been shown to protect against a wide range of pulmonary infections. This broad protection of BCG has been attributed to a memory-like capacity of innate immune cells, termed trained immunity. We have shown that systemic administration of BCG (intravenous) reprograms bone marrow (BM) hematopoietic stem cells (HSCs) to generate trained immunity against *M. tuberculosis*. However, BCG-mediated reprogramming of HSCs cannot be limited to myeloid compartments. In fact, studies in non-human primates suggest BCG can also enhance T cell responses. Thus, considering the critical role of cellular immunity in antiviral responses, we hypothesize that access of BCG to the BM will reprogram lymphoid lineages generating trained T cells that protect against heterologous IAV infection.

To determine the protective effects of BCG against IAV, C57BL/6 mice were vaccinated intravenously (-iv) or subcutaneously (-sc) with BCG (TICE) then infected with H1N1 (PR8). At different timepoints post-infection, mortality, viral burden and cellular immune responses were assessed. By using Rag1<sup>-/-</sup> mice (lacking B and T cells) and adoptive T cell transfer, we aim to address the role of BCG-induced T cell responses in the protection against IAV.

We found that BCG-iv vaccinated mice were protected against IAV infection with a remarkably enhanced survival rate. The protection of BCG-iv against IAV was mediated via adaptive immunity as there was no protection in Rag1<sup>-/-</sup> mice. Specifically, we found a robust increase in a subset of  $\alpha\beta$  memory T cells expressing high levels of CX3CR1 in the blood, with the recruitment of this population into the lung tissue being required for protection. We demonstrate that these CX3CR1<sup>hi</sup> T cells display a unique transcriptional signature indicative of high effector function and mediate protection in a manner independent of antigen-specificity.

These findings collectively indicate that BCG-IV can induce heterologous T cell immunity against IAV infection. Considering the antigen-independent nature of this cross-protection, BCG could thus potentially represent a preventative tool against emergent influenza strains. The present study expands the novel concept of trained immunity to the adaptive immune system whereby lymphocytes could also feature in a first line of defense against an unrelated pathogen.

## Day 2, Poster 31 - The mystery of BCG vaccine in protection against SARS-CoV-2

Kristina Nikolaou<sup>1, 2, 3</sup>, Maziar Divangahi<sup>1, 2, 3</sup>

<sup>1</sup>McGill University, <sup>2</sup>Meakins-Christie Laboratories, <sup>3</sup>Translational Research in Respiratory Diseases Program, Research Institute of the McGill University Health Centre

**Background:** An increasing body of literature indicates that live vaccines, most notably those using the *Mycobacterium* Bacillus Calmette-Guérin (BCG), provides cross-protection against other infectious diseases by inducing memory in innate immune cells, referred to as '*trained immunity*'. We have recently demonstrated that epigenetic reprogramming of hematopoietic stem cells (HSCs) following BCG vaccination generates protective trained immunity against tuberculosis (TB). We have also shown that BCG vaccination provides protection against influenza virus but not SARS-CoV-2. In contrast to our observations, a study by Alan Sher's group showed that BCG vaccination provides protection against SARS-CoV-2. We notice that the major difference between the two studies is the strain of BCG—Pasteur (Sher) vs Tice (our group). The purpose of this study is to determine how BCG Pasteur generates protective trained immunity against SARS-CoV-2

**Methods:** Three groups containing four wild-type C57BL/6 mice each were vaccinated intravenously with either a PBS control,  $1 \times 10^6$  CFU BCG Pasteur obtained from the Sher lab, or  $1 \times 10^6$  CFU BCG Tice from the Divangahi lab. Four weeks after vaccination, the bone marrow was harvested from each mouse and an LKS panel (Lineage<sup>-</sup>cKit<sup>+</sup>Sca-1<sup>+</sup>) was used to assess the levels of HSCs, as well as immune cell progenitors (myeloid, lymphoid, erythroid) for flow cytometry. Bone marrow, spleen, lungs, and liver were also harvested after four weeks. Homogenized organs were diluted and plated on 7H10 supplemented with PANTA to assess differences in dissemination. Mycobacterial growth curves were also used to assess the growth of both BCG Pasteur and Tice.

**Results:** BCG Pasteur and Tice both demonstrated no significant difference in their growth rates. Both strains demonstrated significant expansion when compared to the control group in the LKS cells, as well as the multi-potent progenitors (MPP) and long term-HSCs (LT-HSCs). No significance was seen in the short term-HSCs (ST-HSCs). BCG Pasteur and Tice demonstrated a significant decrease in the common myeloid progenitors (CMP) when compared to the control group, while BCG Pasteur showed a significant decrease in the common lymphoid progenitors (CLP) when compared to the BCG Tice group. BCG Pasteur and Tice also showed similar dissemination to the bone marrow, spleen, and liver, while BCG Pasteur showed greater dissemination to the lungs than BCG Tice.

**Conclusions:** The mechanism of how BCG Pasteur generates protective trained immunity against SARS-CoV-2 is still unclear. It is possible that the increase in dissemination to the lungs, or the lower expression of CLPs may play a role. Pathways involved in the cross-protection against SARS-CoV-2 need to be further investigated to better understand the induction of trained immunity by BCG Pasteur.

# Day 1 Oral - Feasibility of an animated video intervention post-acute exacerbation of COPD

Kriti Agarwal<sup>1</sup>, Matheus de Paiva Azevedo<sup>1</sup>, Jean Bourbeau<sup>2</sup>, Deborah da Costa<sup>2</sup>, Sarah Ahmed<sup>2</sup>, Pauline Anderson<sup>3</sup>, Tania Janaudis-Ferreira <sup>2</sup>

<sup>1</sup>McGill University, <sup>2</sup>CORE, RI-MUHC, <sup>3</sup>RI-MUHC

## Background:

Acceptance and completion rates of pulmonary rehabilitation (PR) after an acute exacerbation of COPD (AECOPD) are remarkably low.

## Aims and objectives:

Our aim was to 1) assess the feasibility and acceptability of delivering a theory and evidence-based intervention: an online animated video about PR to patients during or post AECOPD, 2) evaluate the post- vs pre-video changes in patient knowledge and understanding of PR, readiness and motivation to participate in a PR program.

## Methods:

We conducted a single group pre-post intervention study. The online animated video was shown to participants using a tablet, either at the in-patient respiratory ward or at the clinic. Patients were encouraged to watch the video several times and discuss their participation in PR with their family members. Feasibility measures included recruitment, adherence, and completion rates. Knowledge was evaluated using Understanding COPD (UCOPD) and Bristol COPD Knowledge (BCKQ) questionnaires. Readiness to commence PR was measured by a Readiness to Change Exercise Questionnaire, and a likert-type scale assessed motivation.

## Results:

A total of 52 patients were evaluated, 18 accepted to participate of which 12 completed the intervention. The recruitment, adherence and completion rates were 75%, 67% and 100% respectively. The mean change of the UCOPD was 5.98 and of the BCKQ was -0.25. Nearly 67% of our patients presented readiness to commence PR and reported a mean increase of 7.5 scores on the likert-scale for motivation levels. Ninety-two percent of the included patients would recommend the video to other AECOPD patients.

## Conclusion:

The delivery of the animated video to patients with an AECOPD was feasible, acceptable to patients and improved knowledge and readiness to commence PR.

## Day 2, Poster 18 - BCG-mediated protection against Bladder Cancer via Trained Immunity

Leonardo Jurado<sup>1</sup>, Maziar Divangahi<sup>1</sup>

<sup>1</sup> McGill University, <sup>2</sup> Meakins-Christie Laboratories, <sup>3</sup> Research Institute of the McGill University Health Centre

Bacillus Calmette-Guérin (BCG) is the only available and widely used vaccine against tuberculosis (TB). However, BCG mediates non-specific immunity against several respiratory infections and cancer. For instance, intrabladder (IB) BCG instillations are the gold-standard adjuvant immunotherapy for patients with non-muscle-invasive Bladder Cancer (NMIBC). However, the precise mechanism of action by which BCG induces anti-tumor immunity is still unclear.

Recently we and others have shown that BCG epigenetically reprograms innate immune cells to enhance host protection against both related and unrelated pathogens. This phenomenon has been termed trained immunity (TI). Furthermore, the long-term effects of TI induced by BCG require reprogramming of hematopoietic stem cells (HSC) in the bone marrow (BM). **Therefore, we hypothesize that BCG treatment will induce reprogramming in HSCs, generating TI that will increase the anti-tumoral capacities of innate immune cells against BC.**

To test this hypothesis, we used an orthotopic mouse model, in which 6- to 8-week-old C57BL/6 female mice under anesthesia are instilled with  $8 \times 10^5$  MB49 cancer cells (IB) followed by the treatment of  $5 \times 10^6$  BCG (IB) at different timepoints. Using this mouse model, we demonstrated that BCG treatment of mice with established orthotopic BC, had significantly improved survival rates due to tumor clearance. Mice treated with three BCG IB instillations (days 1, 7 and 14) after tumor implantation exhibited 80% survival. This is consistent with a marked reduction in bladder weight, together with the radiological and histological absence of tumor. By means of immunophenotyping of the BM cells after BCG IB instillations, we observed significant expansion of the hematopoietic stem and progenitor cell populations and Common Lymphoid Progenitor cells (CLP). Together, these data demonstrate the establishment of a robust preclinical murine BC model to investigate the protective mechanisms of IB BCG and strongly support TI as putative mechanism of protection in BC.



## Day 1, Poster 2 - Mechanisms of early life RSV infection-mediated enhancement of Type 2 allergic lung inflammation

Lydia Labrie<sup>1,2</sup>, Rami Karkout<sup>1,2</sup>, Brian Ward<sup>1</sup>, Elizabeth Fixman<sup>1,2</sup>

<sup>1</sup>Research Institute of McGill University Health Centre, <sup>2</sup>Meakins-Christie Laboratories, RI-MUHC, McGill University

Respiratory syncytial virus (RSV) infection leads to millions of hospitalizations and many thousands of deaths per year. Early childhood RSV infection is associated with development of wheezing and asthma. In addition, sex-related disparities exist in asthma epidemiology and morbidity, although the mechanisms are not clear. The prevalence of asthma is greater in boys before puberty, after which prevalence becomes greater in women. Currently, neither antivirals nor vaccines are available for RSV. A better understanding of the mechanisms by which early-life RSV infection can lead to wheezing and asthma later in life would contribute to the development of novel preventative and therapeutic strategies. We have developed a model in which 10-day old mice are infected intranasally with RSV and then exposed acutely to a common allergen, house dust mite (HDM) in order to define how early-life RSV infection modulates Type 2 innate inflammation in response to allergen exposure in the lung. We hypothesize that RSV will enhance HDM-induced lung inflammatory responses more dramatically in female mice and that the effects of RSV will remain long after viral clearance. Our data show that early-life exposure to RSV enhanced Type 2 lung inflammation upon HDM exposure 10 days after viral infection. Enhanced responses were absent in mice exposed to only RSV or HDM. Specifically, we found increased levels of the innate cytokine IL-33 in the lung 6h following HDM exposure only in mice previously infected with RSV. Our data also demonstrate, that eosinophil activation and accumulation of group 2 innate lymphoid cells (ILC2s) in the lung were more prominent in female mice exposed to both RSV and HDM. Moreover, our flow cytometry analysis showed the number of IL13+ T cells (both CD4+ and CD8+) in the lung were significantly increased in mice exposed to both RSV infection and HDM, although the expression of ST2 (the cognate receptor for IL-33) was not linked to T cell cytokine production. These inflammatory responses were maintained when the interval between RSV infection and HDM exposure was extended to one month. In addition, our data show that blocking androgens did not modulate responses in males or females, whereas blocking estrogen receptor (with tamoxifen) reduced the number ILC2s and T cells with the ability to produce IL-13 selectively in female mice. In agreement providing exogenous estrogen enhanced the number of inflammatory cells selectively in male mice (ILC2, CD4+ and CD8+ T cells).

Our results show that early exposure to RSV leads to increased numbers of innate cells as well as T cells in response to a common allergen both when allergen exposure occurs soon after viral infection and when exposure is delayed by several weeks and that most inflammatory responses are enhanced in female mice compared to males. In addition, blocking estrogen receptor masculinizes the female response to RSV→HDM, while providing estrogen feminizes the male response to RSV→HDM. Our work highlights the impact of early-life viral infection and perinatal estrogen on the developing lung, predisposing to enhanced allergic responses long after viral clearance.

## Day 1, Poster 26 - Cannabis Smoke Extract and Cannabis Dry Herb Vapour Induce Inflammation in Lung Epithelial Cells

Maddison Arlen<sup>1, 2, 3</sup>, Emily Wilson<sup>1, 2, 3</sup>, Rui Liu<sup>4</sup>, Cory Harris<sup>4</sup>, David Eidelman<sup>2, 3, 5</sup>, Carolyn Baglole<sup>1, 2, 3, 5, 6</sup>

<sup>1</sup>Department of Pharmacology and Therapeutics, McGill University, Montreal, QC, Canada, <sup>2</sup>Research Institute of the McGill University Health Centre, Montreal, QC, Canada, <sup>3</sup>Meakins-Christie Laboratories, <sup>4</sup>Department of Biology, University of Ottawa, ON, Canada, <sup>5</sup>Department of Medicine, McGill University, Montreal, QC, Canada, <sup>6</sup>Department of Pathology, McGill University, Montreal, QC, Canada

The most common route of cannabis consumption is via inhalation of smoke. When cannabis is burned, cannabinoids, terpenes and a multitude of toxic combustion products are released. These include carcinogens, polycyclic aromatic hydrocarbons, and other pulmonary irritants that exacerbate inflammation. Dry herb vaporizers have been proposed as a safer alternative to smoking cannabis, as they heat the plant materials to release cannabinoids without producing harmful by-products of combustion. However, the safety profile of inhaled cannabis smoke and vapour remains poorly characterized, warranting further investigation in light of their increasing usage. We sought to develop cannabis smoke extract (CaSE) and cannabis vapour extract (CaVE) as in vitro surrogates of pulmonary exposure. The cannabinoids and combustion products were characterized by HPLC and GC/MS respectively. Higher levels of cannabinoids were released via smoking. Both burning and vaporizing cannabis emitted harmful combustion products. Treatment of the human lung epithelial cell line BEAS-2B with CaSE and CaVE for 6 and 24 hours significantly increased *CXCL8*, *CYP1A1* and *NQO1* mRNA levels, indicating a pro-inflammatory response to cannabis smoke and vapour containing the myriad of compounds inhaled by users. Cytokines will be analyzed via ELISA/multiplex assays as an indice for altered immune function. Despite the legalization of cannabis in Canada, the health consequences of inhaled cannabis products are poorly characterized. Further research is vital to ensure the safety of millions of Canadian consumers.

## Day 2, Poster 22 - MicroRNA-155 Modulates IL-13R $\alpha$ Subunits in Bronchial Epithelial Cells in Severe Asthma

Martin Klein<sup>1,2</sup>, Pierre-Alexandre Gagnon<sup>1</sup>, Mabrouka Salem<sup>1</sup>, Mahmoud Rouabhia<sup>3</sup>, Jamila Chakir<sup>1</sup>

<sup>1</sup>Institut Universitaire de Cardiologie et de Pneumologie de Québec, Université Laval, Québec, Canada - Québec (Canada), <sup>2</sup>Institut Universitaire de Cardiologie et de Pneumologie de Québec, Université Laval, Québec, Canada - Québec (Canada), <sup>3</sup>GREB, Faculté de médecine dentaire, Université Laval, Québec, Canada - Québec (Canada)

**Introduction:** Asthma is a chronic disease characterized by inflammation and airway remodeling. microRNAs (miR) were recently shown to participate in asthma physiopathology. miR-155 have been shown to promote Th2 response, ILC2 survival, eosinophilic inflammation and is increased in severe asthma patients' serum. However, its modulation and role in bronchial epithelial cells (BECs) remains unclear in severe asthma.

**Objectives:** To measure the expression of miR-155 in BECs of healthy versus severe asthma patients and to evaluate the effect of miR-155 modulation on BECs behavior and function.

**Methods:** BEC were obtained from bronchial biopsies of severe asthma and healthy donors. miR-155 expression was evaluated by q-PCR in BECs of severe asthma compared to healthy donor. BECs were transfected with miR-155 inhibitor, miR-155 mimic and their respective scrambles. Expression of IL-13R $\alpha$ 1 and IL-13R $\alpha$ 2 and their respective pathways were evaluated by q-PCR and western blots. BECs repair process was determined by mechanical injury.

**Results:** We observed that inhibition of miR-155 is associated with a gene and protein decrease of IL-13R $\alpha$ 1 and an increase of IL-13R $\alpha$ 2. As IL-13R $\alpha$ 2 is known to participate in BECs repair process, we investigated how miR-155 and IL-13R subunits modulate BECs repair. We observed that severe asthma had a delayed repair process compared to healthy BECs. The same experiment was performed with miR-155 inhibitor and mimic transfection. miR-155 overexpression delays BECs wound healing whereas its inhibition enhances this process in both healthy and severe asthma BECs. The delay of BECs repair process is associated with an increase IL-13R $\alpha$ 1/STAT6 and a decrease IL-13R $\alpha$ 2/STAT3/c-Jun pathways. Thus, enhance BECs repair process is associated with a decrease IL-13R $\alpha$ 1/STAT6 and an increase IL-13R $\alpha$ 2/STAT3/c-Jun pathways in both healthy and severe asthma BECs.

**Conclusion:** miRNA-155 is overexpressed in BECs of severe asthma patients and contributes to delay BECs repair process favoring IL-13R $\alpha$ 1 to the detriment to IL-13R $\alpha$ 2 pathway. These results show the crucial role of miR-155 in severe asthma BECs repair.

## Day 2, Poster 29 - Genetic Regulation of the Host Immune Response to *Cryptococcus neoformans* Infection

Marwa El Sheikh<sup>1,2</sup>, Isabelle Angers<sup>1,2</sup>, Salman Qureshi<sup>1,2</sup>

<sup>1</sup>Faculty of Medicine and Health Sciences, Division of Experimental Medicine, Meakins-Christie Laboratories, McGill University, <sup>2</sup>Research Institute of the McGill University Health Center, Montréal, Québec, Canada

Cryptococcosis is an opportunistic pulmonary infection that often progresses to fatal meningitis. Host genetic susceptibility factors for progressive disease remain poorly understood. Genetic analysis of naturally resistant CBA/J mice has validated the role of the *Cnes2B* locus on chromosome 17 as a regulator of susceptibility to progressive cryptococcal disease. Resistant *Cnes2B* sub-congenic mice experience greater morbidity and significantly higher mortality rates compared to susceptible C57BL/6N mice despite their ability to control fungal burden.

We hypothesized that resistant *Cnes2B* mice mount a significantly stronger innate and adaptive immune response compared to C57BL/6N mice following intratracheal *C. neoformans* (*Cn*) infection.

Lung cytokine and chemokine quantification by multiplex immunoassay at serial time points post-infection (p.i) with 10<sup>4</sup> colony forming units of *Cn* 52D revealed significantly higher expression of pro-inflammatory, Type 1-, and Type 3-associated mediators in *Cnes2B* mice with significantly higher expression of Type 2-associated mediators in C57BL/6N mice. Intracellular cytokine staining identified CD4 T cells as the main producers of IFN $\gamma$  and IL-17a. Increased IFN $\gamma$  and IL-17a expression between day 7 and day 14 p.i, coincided with fungal burden control and the onset of morbidity and mortality in *Cnes2B* mice.

Isolation of lung macrophage populations by fluorescence-activated cell sorting and quantification of intracellular fungal burden demonstrated that alveolar macrophages (AMs) are primarily responsible for the initial phagocytosis and containment of *Cn*. *Cnes2B* AMs exhibit greater absolute killing of intracellular *Cn* compared to C57BL/6N AMs; however, relative killing was equivalent between the strains. Further investigations will delineate genetically regulated mechanisms of AM-mediated *Cn* killing.

## Day 2, Poster 5 - Investigating the Role of h-Caldesmon in Smooth Muscle Force Maintenance: Implications for Understanding Smooth Muscle Dysfunction

Matheus Schultz<sup>1,2</sup>, Linda Kachmar<sup>2</sup>, Gijs Ijpma<sup>2</sup>, Anne-Marie Lauzon<sup>1,2,3</sup>

<sup>1</sup>Department of Biomedical Engineering, McGill University, <sup>2</sup>Meakins-Christie Laboratories, <sup>3</sup>Department of Medicine, McGill University

Smooth muscle (SM) is found in most hollow organs of the body and its dysfunction is associated with several diseases such as asthma and hypertension. Nonetheless, the regulation of the SM molecular contractile machinery is still poorly understood. It is known that SM contraction is mainly regulated by phosphorylation of myosin molecular motors, by myosin light chain kinase, and dephosphorylation, by myosin light chain phosphatase (MLCP). However, myosin phosphorylation cannot account for all aspects of SM regulation, as studies have shown decoupling between force and myosin phosphorylation levels during prolonged SM contraction. Hence, actin filament associated proteins are also believed to play a role in SM regulation. Indeed, studies alluded to the involvement of the actin binding protein h-Caldesmon (hCaD) in SM regulation. To gain insight into the role of hCaD on SM force maintenance during myosin dephosphorylation, we injected MLCP during in vitro motility measurements performed in the presence or the absence of hCaD. In line with previous studies, addition of hCaD to in vitro motility assays resulted in a lower average velocity ( $v_{avg}$ ) of moving actin filaments. Sigmoidal fits to the fraction of moving filaments ( $f_{mot}$ ) during myosin dephosphorylation showed an earlier and faster decrease in  $f_{mot}$  in the presence of hCaD. These results agree with previous data obtained at the whole muscle level that showed that hCaD increases the rate of relaxation of arterial SM. They can be explained either by an increased dephosphorylation rate in the presence of hCaD or by an enhanced reattachment of dephosphorylated myosin to actin. Our ongoing molecular force measurements should help elucidate the mechanism by which hCaD regulates SM contraction and shine light into the pathophysiology of SM dysfunction.

## Day 1, Poster 22 - Regulation of the bone marrow iron metabolism in hematopoiesis and host defense against TB

Mina Sadeghi<sup>1,2</sup>, Nargis Khan<sup>3</sup>, Maziar Divangahi<sup>1,2</sup>

<sup>1</sup>Meakins-Christie Laboratories, Department of Medicine, Department of Microbiology and Immunology, McGill University, <sup>2</sup>McGill International TB Centre, McGill University Health Centre, <sup>3</sup>Cumming School of Medicine, University of Calgary

*Mycobacterium tuberculosis* (*Mtb*) is one of the top infectious disease killers worldwide, claiming 1.5 million lives annually. Iron is required by every living organism and *Mtb* obtains iron from its host to survive. We and others have shown that the dysregulation of iron metabolism in the murine model of TB and in patients with active TB promotes dissemination and susceptibility to disease. Yet, the mechanisms of how *Mtb* hijacks host iron metabolism remain largely unknown. In mammals, the vast majority of iron is found in heme, which is packaged into hemoglobin (Hb) within erythroid progenitors during bone marrow (BM) erythropoiesis. During erythropoiesis, lineage-committed progenitors give rise to mature red blood cells (RBCs), which circulate systemically for tissue oxygenation. We have recently shown that an avirulent mycobacteria strain (BCG-vaccine) reprograms hematopoietic stem cells (HSCs) to promote myelopoiesis and enhance immunity (Kaufmann et al. *Cell* 2018) against *Mtb*, while access of a virulent strain of mycobacteria (*Mtb*) to the BM rewires heme metabolism in HSCs to limit myelopoiesis and reduce immunity against TB (Khan et al. *Cell* 2020). In this study, we have found that several erythroid progenitors in the BM were significantly depleted post-*Mtb* infection, and not BCG vaccination. This finding was coincident with a reduction of mature RBCs, Hb and iron in the blood. Moreover, these erythroid progenitors displayed dysregulated iron levels in both intra- and extracellular compartments, uniquely post-*Mtb* infection. These findings provide new insights into the pathogenesis of TB, and highlight a novel targeted host therapy against this devastating disease.

## Day 2, Poster 12 - Association of dysanapsis genetic risk score with airflow obstruction

Motahareh Vameghestahbanati<sup>1,2</sup>, Leina Kindgdom<sup>2,3</sup>, Benjamin Smith<sup>2,4</sup>

<sup>1</sup>Department of Internal Medicine, McGill University Health Center, <sup>2</sup>Meakins Christie Laboratories, <sup>3</sup>College of Medicine, McGill University, <sup>4</sup>Department of General Medicine, Columbia University

**INTRODUCTION:** Dysanapsis refers to a structural mismatch between airway tree and lung size that arises early in life. Dysanapsis assessed by computed tomography (CT) has been shown to be established by early adulthood and is associated with prevalent and incident chronic obstructive pulmonary disease (COPD) later in life. Furthermore, CT-assessed dysanapsis has recently been associated with several genetic polymorphisms in or near genes implicated in lung development. This study tested whether higher dysanapsis genetic risk score (GRS) is associated with airflow obstruction.

**METHODS:** The UK biobank is a national cohort study that included participants from the general population aged 40-69 years and performed spirometry and genotyping. Dysanapsis genetic risk score was computed using genetic polymorphisms identified in a recent genome-wide associated analysis of CT-assessed dysanapsis. The association of dysanapsis genetic risk score with forced expired volume in 1-second (FEV<sub>1</sub>)/forced vital capacity (FEV<sub>1</sub>/FVC), FEV<sub>1</sub>, and with COPD were assessed by fitting regression models adjusted for age, sex, height, principal components of genetic ancestry, cigarette smoking status, pack-years, and asthma diagnosis. Secondary analyses assessed these associations among never smokers and among the youngest age stratum (40-49 years old).

**RESULTS:** Among 420,187 participants with spirometry and genotype data, mean  $\pm$  SD age was 56 $\pm$ 8 years, 54.6% were female, 55.3% reported never smoking, mean  $\pm$  SD FEV<sub>1</sub>/FVC was 0.76 $\pm$ 0.07 and 15.2% had COPD. Compared to participants in the lower decile of dysanapsis genetic risk, those in the highest exhibited lower FEV<sub>1</sub>/FVC (adjusted mean difference: -0.02, 95%CI: -0.02-0.02), lower FEV<sub>1</sub> (adjusted mean difference: -97.6 ml, 95%CI: -110.5, -84.6) and higher odds of COPD (adjusted odds ratio: 1.96, 95%CI: 1.80-2.14). Similar associations were observed among never smoking and among participants 40-49 years old.

**CONCLUSION:** Among adults, dysanapsis genetic risk score was significantly associated with airflow obstruction and COPD at baseline. Dysanapsis genetic risk appears to be a major contributor to chronic obstructive lung disease risk later in life.

# Day 1, Poster 23 - Association of Dysanapsis and Cardiac Function Among older adults

Motahareh Vameghestahbanati<sup>1,2</sup>, Benjamin Smith<sup>2,3,4</sup>

<sup>1</sup>Department of Internal Medicine, McGill University Health Center, <sup>2</sup>Meakins Christie Laboratories, <sup>3</sup>Division of General Medicine, Columbia University, <sup>4</sup>on behalf of investigators from the Multi-Ethnic Study of Atherosclerosis (MESA) Study

**Background** Dysanapsis refers to an anthropometric mismatch of airway tree caliber arising early in life that is common in the general population and is associated all-cause mortality among older adults, including excess mortality from cardiovascular disease. We investigated whether airway dysanapsis was associated with cardiac structure and function among adults free of clinical cardiovascular disease.

**Methods** The Multi-Ethnic Study of Atherosclerosis enrolled adults free of clinical cardiovascular disease aged 45-84 years old from 6 U.S. communities (2000-2002). Dysanapsis was assessed as the mean of airway lumen diameters divided-by cube-root of total lung volume estimated from cardiac computed tomography (airway-to-lung ratio<sub>cardiacCT</sub>); cardiac structure and function (left ventricular mass and ejection fraction) were assessed from cardiac magnetic resonance imaging. Regression models adjusted for anthropometrics, demographics and potential confounders including tobacco smoke, air pollutant exposures and traditional cardiovascular risk factors.

**Results** Among 4,893 participants (mean±SD age: 69±7 years; 52.6% female; 52.1% never-smokers; airway-to-lung ratio<sub>cardiacCT</sub>: 0.024±0.007; left ventricular mass 148.1±39.4 g; left ventricular ejection fraction: 69.1±7.4%), in adjusted models, per 1-SD decrement in airway-to-lung ratio<sub>cardiacCT</sub>, there was +1.04 g increment in left ventricular mass (95%CI: 0.28, 1.80; P=0.007) and -0.23% decrement in ejection fraction (95%CI: -0.44%, -0.02%;P=0.032). Similar results were observed among never-smoking participants.

**Conclusion** Lower airway-to-lung ratio<sub>cardiacCT</sub> was associated with higher left ventricular mass and lower ejection fraction, suggesting that airway dysanapsis is associated with altered cardiac structure and function.



# Day 1, Poster 18 - The Role of the BTLA-HVEM Signaling Axis in Modulating CD4 T Cell and Airway Smooth Muscle Cell Phenotypes

Muyang Zhou<sup>1,2</sup>, Rui Sun<sup>1,2</sup>, James Martin<sup>1,2</sup>

<sup>1</sup>Department of Medicine, Division of Experimental Medicine, McGill University, <sup>2</sup>Meakins-Christie Laboratories, Research Institute of the McGill University Health Centre

**Rationale:** CD4<sup>+</sup> T cells infiltrate the airway smooth muscle (ASM) layer in asthmatics and their interactions may favor persistent airway hyperresponsiveness (AHR) and airway remodeling. We recently observed upregulated B and T lymphocyte attenuator (BTLA) transcription as well as decreased IFN- $\gamma$  synthesis from CD4<sup>+</sup> T cells co-cultured with ASM cells. ASM cells express the BTLA ligand, herpes virus entry mediator (HVEM). *We hypothesized that the immune checkpoint BTLA-HVEM interaction modulates the phenotypes of CD4<sup>+</sup> T cells and ASM cells in co-culture.*

**Methods:** CD4<sup>+</sup> T cells isolated from human peripheral blood were activated with CD3/28 Dynabeads and co-cultured with ASM cells for 24 hours. Following co-culture, BTLA and HVEM on the respective cells and cytokine synthesis from CD4<sup>+</sup> T cells were assessed by flow cytometry. ASM cells were characterized by changes in proinflammatory gene expression via RT-qPCR and STAT1 activation by Western blot.

To further elucidate the role of BTLA-HVEM, stable HVEM knockdown ASM cell lines were generated and co-cultured with activated CD4<sup>+</sup> T cells. Cell phenotypes were assessed by the same methods.

**Results:** BTLA was expressed on  $44.7 \pm 3.55$  % of CD4<sup>+</sup> T cells, but its level was unaltered ( $p = 0.2045$ ) in response to co-culture. IFN- $\gamma$ , IL-10 and IL-17A synthesis from co-cultured CD4<sup>+</sup> T cells were decreased. However, this change was not rescued by disrupting BTLA-HVEM interaction.

Co-cultured ASM cells showed marked upregulation of HVEM, phosphorylated STAT1 as well as IFN- $\gamma$  associated proinflammatory genes, including CXCL9, 10, 11 and ICAM-1. HVEM knockdown partially reversed these changes.

**Conclusions:** Co-culture of CD4<sup>+</sup> T cells and ASM cells resulted in a more quiescent CD4<sup>+</sup> T cell phenotype, while the ASM cells became more pro-inflammatory, presumably due to IFN- $\gamma$ -induced STAT1 signaling. BTLA-HVEM was not responsible for the suppression of cytokine synthesis in co-cultured CD4<sup>+</sup> T cells. However, HVEM signaling in ASM cells supports IFN- $\gamma$ -associated proinflammatory gene expression, the effects of which were disrupted by HVEM knockdown.

## Day 2, Poster 27 - Stimulation of human mucosal B cells with germinal center cytokines results in the generation of IL-10+ regulatory plasmablasts

Nicholas Vonniessen<sup>1</sup>, Orsolya Lapohos<sup>1</sup>, Eisha Ahmed<sup>1</sup>, Jana Abi Rafeh<sup>1</sup>, Gregory Fonseca<sup>1</sup>, Bruce Mazer<sup>1</sup>

<sup>1</sup>Meakins-Christie Laboratories, McGill University, Montreal, QC, Canada

**Background:** The germinal center (GC) is a transient microstructure found within lymphoid tissues that develops following cognate T-B cell interactions. The induction and maintenance of the GC is a highly coordinated process involving multiple cell types and is essential for the generation of high-affinity antibody-producing plasma cells and long-lived memory B cells. Aberrant activation of this response contributes to antibody-mediated pathologies observed in autoimmune disorders and atopic asthma. The ability of B cells to regulate immunity, beyond antibody production, resulted in the classification of a novel subset of B-cells, called regulatory B-cells (Breg). The identification of this subset was initially based on their ability to attenuate inflammation through the production of IL-10. Considering their critical role in promoting peripheral tolerance and suppressing the development of type II inflammatory responses that drive allergic disease, we sought to evaluate whether Th2 GC conditions were capable of inducing the expansion of IL-10+ Breg using human mucosal B cells.

**Methods:** Single-cell RNA-seq (scRNA-seq) datasets (accession numbers: E-MTAB-627 8999, E-MTAB-9003 and E-MTAB-9005) were used to evaluate IL-10 expression by B cells localized within the palatine tonsil. Human tonsillar B cells were isolated by negative selection to obtain purities of 96% CD19+ B cells. B cells were cultured for 2 to 5 days at a concentration of  $2 \times 10^6$  cells/ml in 12-well plates. Cells were stimulated with or without anti-CD40 (1  $\mu$ g/mL, purified from the G28.5 cell line), IL-4 (100 U/mL), IL-21 (50 ng/mL) or CpG ODN 2006 (5  $\mu$ g/mL). For intracellular cytokine detection by flow cytometry, 50ng/ml PMA, 1 $\mu$ g/ml ionomycin and 2M GolgiStop were added for the last 5 h of culture. IL-10 secretion was assessed by ELISA and ELISpot.

**Results:** Stimulation of isolated tonsillar B cells with GC cytokines (CD40+IL-4+IL-21) resulted in a significant increase in both the frequency and number of class-switched plasmablasts (CD27+IgD-CD38+IgM-), which was not observed in other stimulation conditions. Compared to CpG+CD40, a well-cited method for the induction of human regulatory B cells, stimulation with CD40+IL-4+IL-21 resulted in a robust induction of CD19+IL-10+ Breg. Class-switched plasmablasts defined the primary Breg subset within the CD19+IL-10+CD27+IgD- population in response to both CpG+CD40 and CD40+IL-4+IL-21 on Day 2; however, this population persisted until Day 5 only in response to stimulation with CD40+IL-4+IL-21.

**Conclusions:** Results identified CD40+IL-4+IL-21 as a novel highly effective condition for the induction of human regulatory B cells and suggests a role for these cells in the regulation of Th2 GC responses. The induction and maintenance of regulatory plasmablasts in response to GC cytokines raises questions regarding the role of these cells in the suppression of IgE-mediated inflammation and whether a deficiency in this response may contribute to the pathophysiology that characterizes allergic disease.

# Day 2, Poster 13 - AhR Signaling in Macrophages Protects Against Cigarette Smoke-Induced Lung Inflammation

Nicole Heimbach<sup>1, 2</sup>, Jun Ding<sup>1, 3</sup>, David Eidelman<sup>1, 3</sup>, Carolyn Baglole<sup>1, 2, 3, 4</sup>

<sup>1</sup>Research Institute of the McGill University Health Centre, Montreal, QC H4A 3J1, Canada, <sup>2</sup>Department of Pharmacology and Therapeutics, McGill University, Montreal, QC H3G 1Y6, Canada, <sup>3</sup>Department of Medicine, McGill University, Montreal, QC H4A 3J1, Canada, <sup>4</sup>Department of Pathology, McGill University, Montreal, QC H3A 2B4, Canada

**BACKGROUND.** The aryl hydrocarbon receptor (AhR) is a ligand-activated transcription factor that responds to chemicals in cigarette smoke (CS), such as benzo[a]pyrene. Upon agonist binding, AhR is transported to the nucleus and induces transcription of target genes such as cytochrome p450 *CYP1A1*; then, AhR is exported from the nucleus and undergoes proteasomal degradation. Although AhR has been shown to protect the lungs against CS-induced lung inflammation, its mechanism is unclear. We hypothesize that AhR protects against CS through its signaling in macrophages.

**METHODS.** THP-1 monocytes were differentiated into macrophages using phorbol 12-myristate 13-acetate (PMA) and treated with cigarette smoke extract (CSE) or the endogenous AhR agonist 6-formylindolo[3,2-b]carbazole (FICZ). Expression of AhR was assessed via western blot and expression of *CYP1A1* mRNA was assessed via RT-qPCR. In addition, single cell RNA-sequencing (scRNA-seq) data from the lungs of non-smokers and smokers were assessed for AhR-dependent gene expression.

**RESULTS.** THP-1 monocyte differentiation into macrophages increased AhR expression, and treatment with CSE or FICZ decreased AhR expression. However, *CYP1A1* was undetected in THP-1 monocytes and macrophages, both at baseline and after treatment with FICZ or CSE. Consistent with these results, scRNA-seq data demonstrated *AHR* expression across human lung macrophage populations, but *CYP1A1* expression was negligible.

**CONCLUSIONS.** In macrophages, AhR was downregulated after treatment with CSE or FICZ, consistent with the canonical AhR signaling pathway in which AhR nuclear translocation is followed by degradation. However, AhR activation from treatment with CSE or FICZ did not induce *CYP1A1* mRNA, raising the possibility that AhR has unique DNA binding behaviors in macrophages compared to previously studied cell types.

**ACKNOWLEDGMENTS.** Canadian Institutes of Health Research (CIHR), James Frosst Award (McGill University).

# Day 1 Oral - Development of aerosolized pH-switchable lipid nanoparticles for the delivery of nucleic acids for the treatment of lung disease

Paola A. Rojas-Gutierrez<sup>1</sup>, Bellastrid Doran<sup>1</sup>, Sarah Zaidan<sup>1</sup>, Larry C. Lands<sup>1</sup>

<sup>1</sup>Meakins-Christie Labs, Research Institute-McGill University Health Centre

Inhaled therapies are a convenient way to treat lung diseases, such as cystic fibrosis, asthma, and chronic bronchitis. Encapsulation using lipid nanoparticle (LNPs) for transmucosal delivery offers an effective way to deliver therapeutics to lung epithelial cells. However, there are two barriers to overcome to effectively deliver inhaled treatments to airway cells. First, the airway mucus barrier must be penetrated to reach the underlying epithelium. Then cellular uptake and release of the therapy in the cytosol is required for drug delivery or transfection. Cationic pH-switchable lipid (CSL3) has been reported to produce LNPs with endosomal escape for efficient cellular transfection.<sup>1</sup> However, they present reduced mucus penetration due to the positive charge. **We hypothesized** that LNPs with a size of <200 nm and a surface charge close to neutrality will ensure transmucosal transport. **The goal** of this project is the optimization of the physicochemical properties of pH-switchable LNPs to enable aerosolization and pulmonary delivery of nucleic acids to epithelial cells. The optimization of physicochemical properties of LNPs was studied by engineering the lipid formulation. LNPs are composed by four types of lipids: cationic, helper, sterol, and polymeric. LNPs were synthesized by microfluidics, size and surface charge were characterized by dynamic light scattering and zeta-potential. Encapsulation of poly(I:C) or Firefly luciferase (Fluc) reporter mRNA in the LNPs was evaluated using SYBR gold. Aerosolization of LNPs was performed with an electronic micropump nebulizer (Aeroneb Lab). Herein, we studied how the chemical structure of the sterol, helper and polymeric lipids affect the physicochemical properties of pH-switchable LNPs before and after aerosolization. We studied 18 formulations and found that the alkyl length and double bonds of the helper and polymeric lipids are key elements for the aerosolization stability of pH-switchable LNPs. Lipids with short alkyl chains (14C) and unsaturated bonds (1 double bond) increase the stability after nebulization. The best pH-switchable LNP formulation was then tested for translation efficiency on BEAS-2B cell line and NHBE primary cells and compared to free mRNA, commercial transfecting agents (TransIT 2020 and Escort IV), and LNPs formulated with cationic lipid (DOTAP) and ionizable lipid (DODAP). pH-switchable LNPs formulated with the sterol b-sitosterol presented a higher translation of FLuc-mRNA than when formulated with cholesterol. As well this formulation presented the highest translation when compared to free mRNA, TransIT 2020, and the other LNPs. Preliminary studies using 16HBE at the air-liquid interface for cellular differentiation and mucus generation have been performed by the aerosolization of commercial transfecting agents using the Vitrocell device. These results show the importance of the lipid chemical structure to produce robust LNPs formulation for aerosolization and pave the way for the development of aerosolized therapies that could help patients with lung diseases.

# Day 1, Poster 14 - The effect of cannabis-derived terpenes on the innate immune response in the lungs

Patrick Greiss<sup>1,2</sup>, David Eidelman<sup>1,3</sup>, Mark Lefsrud<sup>4</sup>, Carolyne Baglole<sup>1,2</sup>

<sup>1</sup>Meakins-Christie Laboratories, McGill University, <sup>2</sup>Translational Research in Respiratory Diseases, Research Institute of the McGill University Health Centre, <sup>3</sup>McGill, <sup>4</sup>McGill University

**Rationale:** Upwards of 50% of all drugs approved for market since the early 1980s have been derived from compounds found in plants. *Cannabis Sativa* is a flowering plant that produces more than 400 chemical compounds including cannabinoids, flavones, and terpenes. People generally consume cannabis for recreational and medicinal purposes, largely because of the presence of cannabinoids such as THC, which is responsible for its psychoactive effects. However, terpenes represent a broad chemical class containing more than 150 molecules that are responsible for the aroma of cannabis. Terpenes may be anti-inflammatory and work in concert with cannabinoids, but little is currently known about the impact of terpenes in innate immune cell populations and whether terpenes exhibit anti-inflammatory properties. Most people consume cannabis via inhalation of smoke from a joint, as a vapor generated from heating the plant or as an aerosol from cannabis vape distillate cartridges. Cannabis vape distillates contain high concentrations of cannabinoids with terpenes added to reduce viscosity and add flavor. One cell type in the lungs that comes in contact with inhaled compounds present in cannabis are alveolar macrophages. Alveolar macrophages, which patrol the luminal side of the lungs, are important in recycling surfactant and protecting against infectious organisms. We recently published that cannabinoids reduce the inflammatory response of alveolar macrophages, but the impact of terpenes on lung macrophage biology is not known.

**Hypothesis:** I hypothesize that cannabis-derived terpenes will have a protective effect on alveolar macrophages by reducing inflammatory signalling.

**Objective:** This current study aims to investigate how cannabis terpene mix A and B (two commercial cannabis terpene mixtures) modulate lung macrophage function.

**Methods:** Using MH-S cells (a murine alveolar macrophage cell line), the effect of the two terpene mixes on cell viability have been assessed by MTT assay and flow cytometry. Then, the ability of these mixtures in reducing inflammation were assessed in MH-S cells with and without exposure to lipopolysaccharide (LPS; a component of the cell wall of gram-negative bacteria); outcomes thus far have included cytokine mRNA quantification by qPCR. Cytokine analysis via multiplex assay will be investigated next, along with quantification of macrophage phagocytic capability by flow cytometry.

**Results:** Inflammatory cytokine mRNA production by AMs in response to LPS was not significantly affected by either of the terpene mixtures tested at appropriate concentrations.

**Significance:** This study yields important information on the ability of terpenes to modulate alveolar macrophage function. Future directions for this study involve investigating the interaction between cannabinoids and terpenes, referred to as 'the entourage effect', as well as assessment of the effects of terpenes on additional lung cell populations such as epithelial cells. A better understanding of the immunomodulatory abilities of cannabis-derived compounds may yield novel information on why this plant is anecdotally beneficial for treating diverse human diseases.

## Day 2, Poster 21 - A decade later: long term effects of bronchial thermoplasty on airway remodeling

Pierre-Alexandre Gagnon<sup>1</sup>, Andréanne Côté<sup>1</sup>, Martin Klein<sup>1</sup>, Sabrina Biardel<sup>1</sup>, Michel Laviolette<sup>1</sup>, Krystelle Godbout<sup>1</sup>, Ynuk Bossé<sup>1</sup>, Jamila Chakir<sup>1</sup>

<sup>1</sup>Institut universitaire de cardiologie et de pneumologie de Québec, Université Laval, Québec, QC, Canada

**Introduction:** Bronchial thermoplasty (BT) is an endobronchial procedure consisting in the delivery of heat in airways >3mm in diameter. It is an alternative treatment approach preconized in severe asthma patients in which asthma symptoms control cannot be achieved with high regiment pharmacological/biological therapy. BT was shown to induce morphological changes in the bronchial tree such as airway smooth muscle (ASM) and airway nerve fibers ablation along with clinical benefits. It was recently shown that BT-induced clinical benefits may persist for more than ten years, but the persistence of the morphological changes up to this time is currently unknown.

**Objective:** Measure the persistence of BT-induced morphological changes after more than ten years.

**Method:** Ten participants were enrolled at a follow up session occurring ten to fifteen years post-BT (BT10+ cohort). Bronchial biopsies were collected in treated lobes as well as from the untreated right middle lobe (RML). Since no bronchial biopsies were collected prior to BT in this group, we used ASM and clinical data from a group of 13 participants from which biopsies were collected before and at least one year after BT as a comparative cohort. We measured the proportion of the total biopsy area occupied by ASM (ASM % area) using Masson trichrome staining. MUC5AC and S100A family were similarly assessed using immunohistochemistry.

**Results:** At follow up, both cohorts were similar in terms of age, sex ratio, severe exacerbations, spirometry and medication use. Asthma control questionnaires improved in both cohorts. In the BT10+ cohort, ACQ went from  $1.37 \pm 0.20$  to  $0.91 \pm 0.18$  ( $p=0.11$ ) and AQLQ went from  $5.25 \pm 0.37$  to  $6.11 \pm 0.24$  ( $p < 0.01$ ). In the comparative cohort, ACSS, a local ACQ equivalent in which a perfect control is measured by a score of 100%, went from  $74 \pm 6$  to  $87 \pm 5\%$  ( $p<0.01$ ). The ASM % area in the comparative cohort decreased from  $13.16 \pm 1.12\%$  to  $4.59 \pm 0.88\%$  one-year or more post-BT. At their long-term follow-up, the BT10+ cohort exhibited an ASM area of  $4.93 \pm 1.11\%$ , which is similar to the follow-up of the comparative cohort. Furthermore, similar ASM % area was measured in the untreated RML of both cohorts ( $9.44 \pm 1.02\%$  in the BT10+ cohort and  $8.10 \pm 1.40\%$  in the comparative cohort).

**Conclusion:** BT seems capable of long lastingly reversing ASM remodeling along with maintained clinical improvement. It might similarly have as lasting effects on other morphological features.

## Day 2, Poster 28 - Macrophages in the Muscular Dystrophy (mdx) Mouse Diaphragm Are Reprogrammed by the Dystrophic Environment and Almost Entirely of Bone Marrow Origin

Qian Li<sup>1,2</sup>, Jingtao Wang<sup>1,2</sup>, Orsolya Lapohos<sup>1,2</sup>, Jun Ding<sup>1,2</sup>, Basil J Petrof<sup>1,2</sup>

<sup>1</sup>Meakins-Christie Laboratories, Translational Research in Respiratory Diseases Program, Research Institute of the McGill University Health Centre, <sup>2</sup>Respiratory Division, Department of Medicine, McGill University Health Centre

**Background:** Duchenne muscular dystrophy (DMD) is a severe muscle disease caused by the genetic absence of functional dystrophin, resulting in muscle necrosis and wasting. Inflammation plays a significant role in DMD progression, with muscle macrophages (MPs) contributing to inflammation and fibrosis. We previously found that resident MPs in healthy non-dystrophic muscle have both bone marrow-dependent and bone marrow-independent (embryonic) origins. However, the relative contribution of these two origins to the pathological MPs found in DMD muscles is unknown. In addition, the molecular triggers for pathological remodeling of MP subsets within the dystrophic muscle environment remain poorly understood. The global objective of our study was to investigate how the DMD inflammatory environment shapes the origin and molecular phenotype of MPs in the dystrophic diaphragm.

**Hypotheses:** We hypothesized that in muscular dystrophy (mdx<sup>dmd</sup>) mice, the relative contribution of bone marrow-dependent versus bone marrow-independent MPs is altered. We further postulated that bone marrow-dependent MPs from healthy mice, once placed within the DMD environment, undergo rapid reprogramming that provides clues to the early molecular drivers of pathological inflammation in the dystrophic diaphragm.

**Methods:** Chimeric mice were generated in which bone marrow from wild-type (WT) donor mice (CD45.1 allele) was transplanted into bone marrow-ablated (irradiation+busulfan) host WT or mdx mice (both CD45.2 allele); the diaphragm was shielded from irradiation to preserve the local muscle microenvironment. After 8 wks, all diaphragm MPs from WT (n=4) and mdx (n=5) host recipient mice underwent flow cytometry and cell sorting to determine their origin and molecular profile using bulk RNA-seq. Bioinformatic analyses were applied to identify differentially expressed genes (DEGs) and the key transcription factors driving these changes.

**Results:** Approximately 99% of MPs in mdx diaphragms were derived from the bone marrow as compared to 70% in WT diaphragm. Differential gene expression analysis revealed 262 upregulated and 251 downregulated genes in bone marrow-dependent MPs from mdx recipients compared to WT recipients. Gene ontology analysis suggested that upregulated genes were involved in MP immune activation and response, tissue remodeling, and phagocytosis. Transcription factor motif enrichment analysis identified three candidate transcription factors which may play major roles in driving the upregulated DEGs: interferon regulatory factor (IRF) 9, Runx2, and Smad3. Additionally, eight other known motifs were significantly enriched with seven matching transcription factors from the IRF family.

**Conclusions:** These results suggest that bone marrow-dependent rather than embryonic origin MPs play the key role in DMD pathogenesis. Previously normal wild-type bone marrow-derived MPs are rapidly reprogrammed at the transcriptional level by the muscular dystrophy environment in vivo, and several transcription factors involved in innate immunity such as IRFs were identified as potentially novel therapeutic targets for future exploration.

# Day 1, Poster 1 - A Multi-omics Approach Identifies that Human Antigen R (HuR) Controls Multiple Cellular Pathways in Idiopathic Pulmonary Fibrosis (IPF) Pathogenesis

Quazi Sufia Islam<sup>1,2</sup>, Steven K Huang<sup>3</sup>, Dr. David Eidelman<sup>2</sup>, Dr. Carolyn Baglole<sup>1,2</sup>

<sup>1</sup>Department of Pharmacology and Therapeutics, McGill University, Montreal, Canada, <sup>2</sup>Meakins-Christie Laboratories, RI-MUHC, McGill University, <sup>3</sup>Department of Internal Medicine, University of Michigan, Ann Arbor, Michigan, USA

**Rationale:** Idiopathic pulmonary fibrosis (IPF), a chronic and irreversible disease, is characterized by permanent scarring of the lung that results in death from respiratory failure. A key driver of this scarring is the accumulation of myofibroblasts, induced by transforming growth factor  $\beta$  (TGF- $\beta$ ), that produce excessive amounts of extracellular matrix (ECM) proteins. Recently, we showed that human antigen R (HuR) drives the differentiation of normal lung fibroblasts (NLFs) into myofibroblasts in response to TGF- $\beta$ , concomitant with ECM protein production. HuR is an RNA-binding protein that controls numerous cellular functions including differentiation, survival, and proliferation. We hypothesized, dysregulated function of HuR in IPF-LFs drives disease pathogenesis through numerous cellular pathways.

**Methods:** NLFs and IPF-LFs were obtained from the University of Michigan Interstitial Lung Disease Biorepository and cultured under standard conditions. Fibroblasts were treated with TGF- $\beta$  (5 ng/ml) following HuR knockdown with siRNA. Then, RNA-sequencing (RNA-Seq) as well as mass spectrometry (MS)-based proteomics were performed to comprehensively evaluate the changes in HuR-regulated RNA and protein, respectively.

**Results:** RNA-Sequencing and proteomics analysis revealed that in both NLFs and IPF-LFs, HuR controlled numerous genes and proteins involved in pathways associated with ECM organization, and response to wounding pathways implicated in IPF. HuR controls the expression of proteins associated with IPF pathogenesis, including those involved in the ECM (COL1A1), cell survival (IFGBP2), and protein translation (EIF4) in response to TGF- $\beta$ . Finally, HuR controls numerous non-coding RNA (ncRNA) including LINC00630, involved in cell proliferation.

**Conclusions:** This study provides novel information about many established and novel pathways being regulated by HuR in lung fibroblasts under myofibroblast differentiating conditions identifying HuR as a driver of multiple pathways in IPF.



## **Day 2, Poster 7 - Impact of trigeminal and/or olfactory nerve stimulation on measures of inspiratory neural drive: Implications for breathlessness**

Rachelle Aucoin<sup>1</sup>, Hayley Lewthwaite<sup>2</sup>, Magnus Ekstrom<sup>3</sup>, Andreas von Leupoldt<sup>4</sup>, Dennis Jensen<sup>1,5</sup>

<sup>1</sup>Clinical Exercise & Respiratory Physiology Laboratory, Department of Kinesiology and Physical Education, McGill University, 475 Pine Avenue West, Montréal, Quebec H2W 1S4, Canada, <sup>2</sup>College of Engineering, Science and Environment, School of Environment & Life Sciences, The University of Newcastle, 10 Chittaway Road, Ourimbah, NSW 2258, Australia, <sup>3</sup>Department of Respiratory Medicine, Allergology and Palliative Medicine, Institution for Clinical Sciences in Lund, Lund University, SE-221 00 Lund, Sweden, <sup>4</sup>Health Psychology, University of Leuven, Tiensestraat 102 Box 3726, 3000 Leuven, Belgium, <sup>5</sup>Research Institute of the McGill University Health Centre, Translational Research in Respiratory Diseases Program and Respiratory Epidemiology and Clinical Research Unit, 2155 Guy Street Suite 500, Montréal, Quebec H3H 2R9, Canada

The perception of breathlessness is mechanistically linked to the awareness of increased inspiratory neural drive (IND). Stimulation of upper airway cold receptors on the trigeminal nerve (TGN) with TGN agonists such as menthol or cool air to the face/nose has been hypothesized to reduce breathlessness by decreasing IND. The aim of this systematic scoping review was to identify and summarize the results of studies in animals and humans reporting on the impact of TGN stimulation or blockade on measures of IND. Thirty-one studies were identified, including 19 in laboratory animals and 12 in human participants. Studies in laboratory animals consistently reported that as TGN activity increased, measures of IND decreased (e.g., phrenic nerve activity). In humans, stimulation of the TGN with a stream of cool air to the face/nose decreased the sensitivity of the ventilatory chemoreflex response to hypercapnia. Otherwise, TGN stimulation with menthol or cool air to the face/nose had no effect on measures of IND in humans. This review provides new insight into a potential neural mechanism of breathlessness relief with selected TGN agonists.

## **Day 1, Poster 8 - Impact of trigeminal nerve and/or olfactory nerve stimulation on activity of human brain regions involved in the perception of breathlessness**

Rachelle Aucoin<sup>1</sup>, Hayley Lewthwaite<sup>2</sup>, Magnus Ekstrom<sup>3</sup>, Andreas von Leupoldt<sup>4</sup>, Dennis Jensen<sup>1,5</sup>

<sup>1</sup>Clinical Exercise & Respiratory Physiology Laboratory, Department of Kinesiology and Physical Education, McGill University, 475 Pine Avenue West, Montréal, Quebec H2W 1S4, Canada, <sup>2</sup>College of Engineering, Science and Environment, School of Environment & Life Sciences, The University of Newcastle, 10 Chittaway Road, Ourimbah, NSW 2258, Australia, <sup>3</sup>Department of Respiratory Medicine, Allergology and Palliative Medicine, Institution for Clinical Sciences in Lund, Lund University, SE-221 00 Lund, Sweden, <sup>4</sup>Health Psychology, University of Leuven, Tiensestraat 102 Box 3726, 3000 Leuven, Belgium, <sup>5</sup>Research Institute of the McGill University Health Centre, Translational Research in Respiratory Diseases Program and Respiratory Epidemiology and Clinical Research Unit, 2155 Guy Street Suite 500, Montréal, Quebec H3H 2R9, Canada

Breathlessness is a centrally processed symptom, as evidenced by activation of distinct brain regions such as the insular cortex and amygdala, during the anticipation and/or perception of breathlessness. Inhaled L-menthol or blowing cool air to the face/nose, both selective trigeminal nerve (TGN) stimulants, relieve breathlessness without concurrent improvements in physiological outcomes (e.g., breathing pattern), suggesting a possible but hitherto unexplored central mechanism of action. Four databases were searched to identify published reports supporting a link between TGN stimulation and activation of brain regions involved in the anticipation and/or perception of breathlessness. The collective results of the 29 studies demonstrated that TGN stimulation activated 12 brain regions widely implicated in the anticipation and/or perception of breathlessness, including the insular cortex and amygdala. Inhaled L-menthol or cool air to the face activated 75% and 33% of these 12 brain regions, respectively. Our findings support the hypothesis that TGN stimulation contributes to breathlessness relief by altering the activity of brain regions involved in its central neural processing.

# Day 1, Poster 16 - Isolating the Contribution of Type 2 Immune Effectors in Asthma: IL-13, IL-5, IL-4, and ILC2s

Rafael Intrevado<sup>1,2</sup>, Linda Kachmar<sup>2</sup>, Rami Karkout<sup>2</sup>, Elizabeth Fixman<sup>1,2</sup>, Anne-Marie Lauzon<sup>1,2</sup>

<sup>1</sup>Division of Experimental Medicine, Department of Medicine, McGill University. , <sup>2</sup>Meakins-Christie Labs, Research Institute of the McGill University Health Center.

## Background:

Asthma is a heterogeneous condition characterized by an excessive bronchoconstrictive response to benign stimuli called airway hyperresponsiveness (AHR). Most cases of asthma are provoked by an antigen which elicits the rise of a dysregulated type 2 immune response, the immunity associated with other often overlooked allergic and helminthic diseases. Historically, asthma was thought to be mediated by the classical culprits of T<sub>H</sub>2 cells, eosinophils, and IgE, but a possible upstream controller of this triad has been identified in the recent discovery of the group 2 innate lymphoid cells (ILC2s). As a major producer of type 2 cytokines, ILC2s can regulate T cell activation and IgE class-switching through IL-4 production; coordinate eosinophilia by secreting IL-5; and via its most abundantly secreted cytokine, IL-13, ILC2s can induce AHR. However, whether IL-4, IL-5, IL-13, and ILC2s can have a direct effect on airway smooth muscle (ASM) to induce hypercontractility is still unknown. We hypothesize that pulmonary ILC2s accentuate the contractile properties of ASM and contribute to bronchoconstriction. Our preliminary data report the effects of IL-13 on the contractile properties of asthmatic and control ASM.

## Methods:

We obtained transplant-grade control and asthmatic lungs from a partnership with the American organ recovery agencies IIRAM and NDRI, and we cryo-preserved intrapulmonary bronchi of the 6<sup>th</sup> to 8<sup>th</sup> generations. To perform muscle mechanic experiments, we thawed these airways and finely dissected ASM strips removing the epithelium and connective tissues. Each strip was hooked to a length-controller and force transducer inside an organ bath to measure the force and shortening velocity of the tissues at their baseline. Individual ASM strips were then incubated in 2% FBS DMEM alone, or with IL-5, IL-13, or HCl vehicle. After a 24hr incubation, the muscle mechanics measurements were repeated.

## Results:

Our preliminary data on ASM from control subjects showed a significantly greater force response to methacholine when incubated with IL-13 compared to vehicle control, ( $10.24\% \pm 2.29$  vs  $-16.39\% \pm 5.77$ ,  $p=0.02$ ). (Note that the negative value is due to a decrease in force with time). Similarly, when stimulated with histamine the force increased by  $51.90\% \pm 21.23$  when the ASM was incubated with IL-13 and by  $3.26\% \pm 4.33$ , when incubated with vehicle control, although this difference did not reach significance.

Furthermore, our data on ASM from asthmatic subjects showed a tendency towards a greater force response to methacholine when incubated with IL-13 compared to DMEM ( $4.78\% \pm 8.08$  vs  $-16.20\% \pm 10.24$ ). Similarly, when stimulated with histamine, the force increased by  $21.71\% \pm 10.79$  when incubated with IL-13 compared to a decrease of  $26.39\% \pm 18.46$  when incubated in DMEM.

These data suggest that IL-13 potentiates the force generation by methacholine and histamine in both asthmatic and control ASM. The disproportionate force increase in response to histamine challenge with respect to methacholine suggests that IL-13 may induce a change in contractile or signaling machinery that is histamine-specific. More data acquisition is underway.

# Day 1, Poster 17 - The Impact of Vaporized Cannabis Distillates on Pulmonary Immune Modulation

Roham Gorgani<sup>1, 2, 3, 4</sup>, Valerie Orsat<sup>3, 5</sup>, David Eidelman<sup>3, 4, 6</sup>, Carolyn Baglole<sup>1, 2, 3, 4, 6</sup>

<sup>1</sup>Research Institute of the McGill University Health Centre, <sup>2</sup>Department of Pathology, <sup>3</sup>McGill University, <sup>4</sup>Meakins-Christie Laboratories, <sup>5</sup>Department of Bioresource Engineering, <sup>6</sup>Department of Medicine

**Background:** With the legalization of cannabis occurring throughout the world, its use is increasing. The primary route of cannabis consumption is smoking dried cannabis in the form of a joint. However, cannabis vape cartridges, which utilize battery-powered devices to heat and aerosolize cannabis-derived liquids, are becoming increasingly popular. These cartridges contain cannabis distillates which are extracted from the dry flower. Extraction of these distillates creates a liquid containing high concentrations of cannabinoids such as tetrahydrocannabinol (THC). Despite their growing popularity, the effects of inhaled cannabis distillates on the respiratory tract are not known. Therefore, the purpose of this study was to address this gap in knowledge by creating a standardized mouse model for vaporized cannabis distillate exposure to test the pulmonary immune response upon inhalation.

**Hypothesis:** An acute exposure to vaporized THC distillate will modulate innate pulmonary immune cell populations.

**Methods:** C57BL/6 mice were subjected to a nose-only exposure of vaporized THC distillate using the SCIREQ inExpose and a 510 Thread Cartridge device. A dose response to increasing exposure length and intensity was characterized with 10, 20 and 30-minute exposures at 1 puff per minute, or 1, 2, and 4 puffs per minute exposures for 10 minutes, respectively. Blood was collected immediately following the exposures and serum THC-COOH levels were measured using a THC Forensic ELISA kit. To assess the immunological effects, C57BL/6 mice were subjected to an acute 3-day nose-only exposure of vaporized THC distillate. Lung tissue was collected immediately following the exposure and innate immune cell populations were quantified using flow cytometry.

**Results:** There was a time-dependent increase in blood THC levels, with a concentration of 20.5 ng/mL following a 10-minute exposure and 28.9 ng/mL following a 30-minute exposure. There was also a dose-dependent increase with concentrations of 13.8 ng/mL at 1 puff per minute and 29.1 ng/mL at 4 puffs per minute. In mice exposed to vaporized THC distillate for three days, there were significant increases in lung monocytes and eosinophils compared to mice exposed to air. No significant changes were observed in lung neutrophil, macrophage, or dendritic cell populations.

**Significance:** This research is the first to investigate how inhalation of vaporized cannabis distillates impacts immunomodulation in the lungs. The development of this preclinical model will allow for further investigation of the pulmonary and systemic responses to inhaled cannabis vape distillates. This will be important as the cannabis marketplace continues to grow, and there is a need to understand the safety of new products.

# Day 2, Poster 10 - Role Of Interleukin-33 (IL-33) In Influenza A Induced Airway Hyperresponsiveness In C57BL/6 Mice

Rohin Chakraborty<sup>1</sup>, Julia Chronopoulos<sup>2</sup>, Rui Sun<sup>2</sup>, James Martin<sup>3,4</sup>

<sup>1</sup>Department of Physiology, McGill University, <sup>2</sup>Division of Experimental Medicine, McGill University,

<sup>3</sup>Department of Medicine, McGill University, <sup>4</sup>Meakins Christie Laboratories, Research Institute of the McGill University Health Centre

## Rationale

Seasonal Influenza A infections (IAV) are a threat to asthma sufferers. IAV triggers the release of an epithelial-derived alarmin, IL-33 which contributes to the development of airway hyperresponsiveness (AHR). The pathophysiological mechanism underlying IAV-induced AHR and the link to IL-33 during early IAV infection are not well elucidated. The purpose of this study was to characterize the innate immune response triggered by IAV and elucidate its dependence on IL-33. To do this, we examined the effect of the inhibition of IL-33 signalling by targeting its receptor, ST2 with a neutralizing antibody and observed changes to IAV induced AHR. In addition, we also wanted to elucidate if any modulations to IL-33-driven AHR were mediated by IL-13, a cytokine downstream of IL-33 with strong associations with airway hyperreactivity.

## Methods

PR8 mouse-adapted H1N1 IAV (50 PFU sub-lethal dose), 10 ug anti-ST2 and isotype control IgG antibodies were delivered intranasally to 8-12-week-old female wild-type C57BL/6. The antibodies were administered one day before and 1 day post infection (dpi). Measurements of respiratory mechanics following aerosol challenges of contractile agonist, methacholine (0, 6.25, 12.5, 25 and 50 mg/mL) were used to assess AHR 3 dpi at peak viral replication. Bronchoalveolar lavage (BAL) fluid was assayed for a differential cell count of inflammatory cells and for IL-13 levels. Flow cytometry was conducted to assess innate lymphoid cells (ILCs) and M1/M2 macrophage populations.

## Results

IAV anti-ST2 treated mice had lower respiratory resistance ( $p \leq 0.005$ ) and elastance ( $p \leq 0.01$ ) following inhalation of methacholine compared to its IgG IAV control. Anti-ST2 did not significantly affect IAV induced neutrophils, macrophages and lymphocytes in BAL fluid. IAV does not significantly induce ILCs 3 dpi. The monocyte derived macrophages showed the highest percentage of ST2+ cells. Anti-ST2 treatment reduced both absolute numbers of monocytic derived macrophages ( $p < 0.05$ ) and its M2 population ( $p < 0.01$ ). IAV infected anti-ST2-treated mice compared to IgG IAV control had no difference in BAL-13 levels.

## Conclusion

IAV induced IL-33 initiates an innate immune response that causes AHR independent of the IL-33/IL-13 axis. Anti-ST2 affects the recruitment of monocytes/macrophages that we postulate are responsible for reduced AHR.

## **Day 2 Oral - Elk-1-myocardin cross-inhibition determines the airway smooth muscle phenotypic polarization only when serum response factor is in low abundance.**

Rui Sun<sup>1,2</sup>, Alice Pan<sup>2</sup>, Anne-Marie Lauzon<sup>1,2</sup>, James Martin<sup>1,2</sup>

<sup>1</sup>Meakins-Christie Laboratories, Research Institute of the McGill University Health Centre (RI-MUHC), Montreal, QC, <sup>2</sup>McGill University, Montreal, QC

**Background:** The aberrant changes in smooth muscle contractile and proliferative functions are associated with the pathogenesis of several pulmonary and cardiovascular diseases. The molecular mechanism underlying the smooth muscle contractile versus proliferative phenotypic dichotomy involves two distinct set of genes differentially regulated by the same DNA-binding protein, serum response factor (SRF). Existing evidence suggests the growth-related transcription factor elk-1 and the myogenic transcription factor myocardin (MyoCD) compete for SRF binding to initiate their respective transcriptional activities, thereby mediating smooth muscle phenotypic polarization. The inhibition of MyoCD activity by elk-1 is often observed with the loss of contractility of smooth muscle upon exposure to inflammatory mediators and growth factors in the pathological context. However, whether upregulation of MyoCD inhibits elk-1 and cellular proliferation remains uncertain and was the question addressed in this study. To do so, we generated human airway smooth muscle cell (ASMC) cultures with stable overexpression of MyoCD and assessed its impact on cellular contractile and proliferative properties.

**Methods:** ASMCs were transduced with lentiviral vectors carrying MyoCD, or red fluorescent protein (RFP) as a control, under a CMV promotor, along with a puromycin resistance gene for the selection of successfully transduced cells. Smooth muscle gene expression was measured by qRT-PCR and Western blot (WB). Cellular force generation following agonist challenges was assessed by collagen contraction assay, and quantification of myosin light chain (MLC) phosphorylation as a surrogate readout. Cellular proliferation was assessed by quantifying Ki-67+ cells via flow cytometry and cell count. SRF-elk-1 association was assessed by co-immunoprecipitation.

**Results:** Successful MyoCD transduction was confirmed by an increase in its transcript, and by the upregulation of contractile genes including  $\alpha$ -smooth muscle actin ( $\alpha$ -SMA), myosin heavy chain 11 (MYH11) on both transcript and protein levels. MyoCD-transduction conferred increased cellular force generation reflected by elevated levels of collagen gel contraction and MLC phosphorylation. Total MLC level was also increased in MyoCD-transduced cells. ASMC proliferation, and elk-1-SRF association induced by epidermal growth factor (EGF), but not fetal bovine serum (FBS), was inhibited by MyoCD transduction. Similarly,  $\alpha$ -SMA expression was inhibited by EGF but not FBS. Intriguingly, FBS caused a marked upregulation of SRF, which potentially eliminated the competition for binding between MyoCD and elk-1.

**Conclusion and significance:** The elevated ASMC force generation following MyoCD transduction is due to increased presence of contractile elements, rather than changes in contraction-associated signaling. A limiting quantity of SRF protein is a prerequisite for MyoCD-elk-1 cross-inhibitory mechanism, as excess SRF allows dual activation of proliferative and contractile gene transcription. Clinically, this signifies that an upregulation of SRF could be especially detrimental for promoting pathological changes in smooth muscle, and that SRF could be a promising therapeutic target for ameliorating said changes.

# Day 2, Poster 26 - Deep-learning-based Transposons Expression Quantification in scRNA-seq and scATAC-seq

Ruohan Wang<sup>1,2</sup>, Yumin Zheng<sup>2,3</sup>, Jun Ding<sup>2,4</sup>

<sup>1</sup>McGill University, <sup>2</sup>Meakins-Christie Laboratories, <sup>3</sup>Quantitative Life Sciences, McGill University, <sup>4</sup>Department of Medicine, McGill University

**Rationale:** Transposable Elements (TEs) are important for genomic regulation, evolution, and disease progression, but quantifying them is challenging due to their repetitive nature. In this study, we proposed a deep learning-based model that uses unique and multi-mapping reads to quantify TE expression in single-cell sequencing data.

**Methods:** This study proposed a deep learning-based model to improve the quantification of TEs in single-cell sequencing data. The model consists of an autoencoder and a multi-layer perception (MLP) that use unique mapping, and multi-mapping reads to profile the mapping results on TE regions. By assuming that reads within the same genomic region have a similar distribution, the model uses the distribution pattern of unique mapping reads to distribute the multi-mapping reads. TE family information is also incorporated into the model to help distinguish feature differences between TE families. The MLP is trained to learn the proportion of multi-mapped reads falling in individual TE regions, which enables more accurate TE expression analysis.

**Results:** Our model provides a new tool for exploring the role of TEs in gene regulation and disease. The methods quantifying transposable elements (TEs) expression in single-cell sequencing data were applied to scRNA-seq data, resulting in better clustering than gene expression. We generated a cell-TE count matrix combined with a cell-gene count matrix and identified marker TEs highly expressed in each cell type cluster and TEs that help distinguish clusters. Our methods are also valid for quantifying TE expression in scATAC-seq data. The comparison of clustering results highlights the importance of considering TEs in single-cell analysis.

**Conclusion:** Our model quantifies transposable elements (TEs) expression in single-cell data and improves cell clustering results by incorporating TE expression data into gene expression data. We identify marker TEs for each cell type cluster and TEs that help distinguish clusters, providing new insights into the role of TEs in gene regulation and cellular heterogeneity, which could advance the understanding of the role of TEs in disease.

# Day 2, Poster 32 - Mechanical Ventilation and Resumption of Spontaneous Breathing Do Not Induce Inflammatory Cell Infiltration of the Diaphragm

Ryann Lang<sup>1,2</sup>, Feng Liang<sup>1,2</sup>, Basil J Petrof<sup>1,2</sup>

<sup>1</sup>Meakins-Christie Laboratories, Translational Research in Respiratory Diseases Program, Research Institute of the McGill University Health Centre, <sup>2</sup>Respiratory Division, Department of Medicine, McGill University Health Centre

**Background:** Mechanical ventilation (MV) is a medical intervention that assumes the work of breathing normally performed by respiratory muscles. This leads to inactivity and weakness of the diaphragm, a condition referred to as ventilator-induced diaphragmatic dysfunction (VIDD). Previous work has demonstrated upregulation of proinflammatory mediators and increased oxidative stress in the diaphragm after prolonged MV. In addition, involvement of innate immunity has been suggested by the fact that abrogation of Toll-like receptor 4 signaling or treatment with corticosteroids mitigates VIDD in animal models. The primary objective of this study was to assess the impact of MV on innate immune cells within the diaphragm in a mouse model of VIDD.

**Hypothesis:** We hypothesized that there is increased recruitment of innate immune cells to the diaphragm during MV. Furthermore, it was also postulated that after cessation of MV and the resumption of normal breathing, there would be a further increase in inflammatory cell numbers within the diaphragm due to reloading of the muscle.

**Methods:** Adult male B16 mice (8-13 weeks old, n=5-13 per group) were randomly assigned to either MV or normal breathing (CTRL) groups. The MV group was ventilated for 6 hours and sacrificed: 1) immediately following MV, 2) 24 hours after cessation of MV, or 3) 48 hours after cessation of MV. Diaphragm and limb muscles were removed and flow cytometry was used to quantify monocytes, macrophages and neutrophils in these muscles.

**Results:** As compared to CTRL group mice not exposed to MV, there were no significant differences in either the absolute numbers or percentages of monocytes, macrophages, and neutrophils in the diaphragms of MV-exposed groups. This was the case both immediately following MV and after either 24 hours or 48 hours of diaphragm reloading.

**Conclusions:** In a mouse model of VIDD, there was no evidence for acute inflammatory cell infiltration of the diaphragm either immediately after MV or within 48 hours of resuming normal spontaneous breathing.



## Day 2, Poster 9 - The Impact of Smoking in CFTR Heterozygotes on The Frequency of Pulmonary Exacerbations in COPD

Sahar Mikaeeli<sup>1, 2, 3</sup>, Dr. Simon Rousseau<sup>1, 2, 3</sup>, Dr. Jean Bourbeau<sup>2, 3</sup>

<sup>1</sup>Meakins-Christie Laboratories, <sup>2</sup>Translational Research in Respiratory Diseases, Research Institute of the McGill University Health Centre, <sup>3</sup>mcgill University

Chronic Obstructive Pulmonary Disease (COPD) is the 4th leading cause of mortality and is characterized by accelerated lung function decline. The pathogenesis of COPD is complicated, but cigarette smoking is known as the most important risk factor associated with COPD. The disease progression is associated with acute exacerbations of COPD (AECOPD) leading to increased mortality and frequent hospitalizations. Over the last decade, many investigations showed that cigarette smoke impairs Cystic Fibrosis Transmembrane Conductance Regulator (CFTR) activity and function leading to CFTR dysfunction in COPD patients and affecting the disease severity and progression. Previously, Dr. Rousseau's team studied the relationship between single nucleotide variants (SNVs) in CFTR using a Genome-wide association study (GWAS) in participants with a history of never-, former- and current smoking, and the circulating proteome using data from the Biobanque québécoise de la COVID-19 (BQC19). These preliminary data show five protein Quantitative Trait Locus (pQTL) between three CFTR variants and circulating proteins that could be involved in exacerbation. We hypothesize that the presence of CFTR heterozygotes may alter susceptibility to cigarette smoke and induce CFTR dysfunction and may affect the frequency of pulmonary exacerbations in COPD patients. To investigate our hypothesis, we will use two cohorts including the Quebec lung cancer screening cohort and CanCOLD (Canadian Cohort Obstructive Lung Disease). We will measure circulating biomarkers of inflammation/disease activity that will be used to cluster participants into subgroups sharing similar molecular profiles (endophenotypes). Each endophenotype will be then tested for its association with the frequency of exacerbations and clinical variables. We will measure the protein levels of the 5 pQTLs in our subgroups classified based on the 3 SNPs on CFTR and the Smokers and never-smokers. Likewise, an *in vitro* model in Human epithelial cell lines stimulated by Cigarette smoke extract (CSE) will be used to study the CFTR SNPs and the effect of smoking on CFTR function and dosage. We will further check for the expression of markers of inflammation and the production of oxidative stress markers. Findings from this study will improve early detection of long-term complications in pulmonary exacerbation COPD screening programs in the addition of circulating proteomic data that could further improve the identification of who could benefit from follow-ups.

**Keywords:** COPD, exacerbation, CFTR, Smoking, genetic and environmental risk factors

## Day 2, Poster 14 - Monitoring the Regulation of Mitophagy in Skeletal Muscles Under Normal and Pathological Conditions

Sami Sedraoui<sup>1,2</sup>, Basil J Petrof<sup>1,2</sup>, Sabah Hussain<sup>1,2,3</sup>

<sup>1</sup>Meakins-Christie Laboratories, Translational Research in Respiratory Diseases Program, Research Institute of the McGill University Health Centre, <sup>2</sup>Respiratory Division, Department of Medicine, McGill University Health Centre, <sup>3</sup>Department of Critical Care, McGill University Health Centre

**Background:** The elimination of damaged and dysfunctional mitochondria by the autophagy-lysosome pathway, a process known as mitophagy, is essential for maintaining mitochondrial quality and cellular function. This process has been well characterized in vitro but has been difficult to quantify in vivo. Recently, a fluorescent reporter system called mito-QC (mitochondrial quality control) has been developed to specifically monitor mitophagy in vivo. Mito-QC transgenic mice express a pH-sensitive mitochondrial reporter (mCherry-GFP tag) in which the GFP signal (but not mCherry) is quenched upon mitochondrial delivery to acidic lysosomes. The objective of this study was to employ this new tool to quantify mitophagy in the diaphragm and other skeletal muscles under basal conditions and in response to different catabolic stimuli.

**Methods:** 1) In Vitro Model: Myogenic precursor (satellite) cells were isolated from the diaphragms of mito-QC mice and differentiated into myotubes prior to treatment with a mitochondrial uncoupler, CCCP, to induce mitophagy. 2) In Vivo Models: (a) Hindlimb muscles of mito-QC mice (n=4) were injected with CCCP; (b) Sepsis was induced in mito-QC mice (n=7) by systemic injection of lipopolysaccharide (LPS, 10 mg/kg); (c) Ventilator-induced diaphragm dysfunction (VIDD) was induced in mito-QC mice (n=4) by 6 hrs of mechanical ventilation. The GFP- and mCherry-positive organelles in cells and muscle tissues were counted using confocal microscopy to quantify mitochondria and mitolysosomes, respectively.

**Results:** At baseline, oxidative muscles (diaphragm and soleus) had higher GFP signals and lower mCherry signals than glycolytic muscles, suggesting greater levels of mitophagy in the latter. Treatment of myotubes with CCCP led to a decrease in mitochondrial content with an increase in the relative number of mitolysosomes, and similar findings were observed after intramuscular injection of CCCP in vivo. However, neither sepsis (48 hrs post-LPS) nor VIDD (6 hrs of mechanical ventilation) produced evidence of mitophagy induction within the diaphragm or hindlimb muscles.

**Conclusions:** Our study shows the feasibility of visually quantifying mitophagy in the diaphragm and other skeletal muscles in vivo and in vitro using mito-QC transgenic mice. Although both sepsis and prolonged mechanical ventilation are known to induce general autophagy in the diaphragm, neither of these catabolic conditions increased mitophagy. This suggests that general autophagy and mitophagy are differentially regulated. We speculate that insufficient mitophagy in sepsis or during prolonged mechanical ventilation could play a role in the development of muscle weakness and wasting in these conditions by allowing the accumulation of damaged mitochondria.

## Day 2, Poster 20 - Rheological studies in muco-obstructive lung disease: development of artificial mucus

Smriti Suresh<sup>1,2</sup>, Paola A. Rojas-Gutierrez<sup>1,2</sup>, Larry C. Lands<sup>1,2</sup>

<sup>1</sup>Meakins-Christie Labs, Research Institute-McGill University Health Centre, <sup>2</sup>McGill University

Muco-obstructive lung diseases like primary ciliary dyskinesia (PCD) and cystic fibrosis cause impaired mucociliary clearance. Mucus, a cross-linked network of hydrated mucin glycoproteins along with lipids, DNA, and salts secreted in the airways is transported by the ciliated airway epithelia. Excessive sputum or pathologic mucus with altered rheological properties blocks the airways of patients suffering from these diseases. Expecterated mucus from patients is ideal for investigating treatment strategies. However, the collection of samples especially from pediatric patients, the availability of patients, insufficient amount of sample, and inter-subject variability are some of the challenges. Relying mainly on access to patient sputum samples makes it difficult to develop novel therapies, such as mucolytic or mucus-penetrating aerosol therapies. This lead to the investigation into mucus-mimetic models. Existing models do not accurately mimic the biochemical and bulk viscoelastic properties of sputum. An artificial mucus model was prepared and optimized using a cross-linking agent forming disulphide linkages between mucin proteins along with other components to resemble the chemical composition of real mucus. The viscoelastic properties (elastic ( $G'$ ) and viscous moduli ( $G''$ )) of different formulations were characterized using rheology through a strain sweep test. A formulation with comparable rheological properties ( $G' = 12.73 \pm 2.01$  Pa and  $G'' = 3.37 \pm 0.33$  Pa) to that of PCD patient sputum ( $G' = 0.75-7.92$  Pa and  $G'' = 0.30-2.61$  Pa) was produced. We employed this formulation for preliminary nanoparticle and mucolytic drug studies. Twenty-one percentage of 200 nm green fluorescent nanoparticles were observed to penetrate through artificial mucus. The rheological properties of the artificial mucus formulation were seen to decrease on addition of the mucolytic drug. The disulphide bonds in artificial mucus similar to that of real mucus are broken down by the mucolytic drug leading to lower rheological properties. These results demonstrate the development of a mucus model comparable to patient mucus and pave the way for further investigations of potential treatment strategies for muco-obstructive diseases.

# Day 1, Poster 19 - Pulmonary Toxicity of E-cigarettes in a Murine Model of Allergic Asthma

Sofia Paoli<sup>1, 2, 3</sup>, David H. Eidelman<sup>1, 3, 4</sup>, Carolyn J. Baglole<sup>1, 3, 4</sup>

<sup>1</sup>Research Institute of the McGill University Health Centre, Montreal, QC, Canada , <sup>2</sup>Department of Pharmacology and Therapeutics, McGill University, Montreal, QC, Canada , <sup>3</sup>Meakins-Christie Laboratories, <sup>4</sup>Department of Medicine, McGill University, Montreal, QC, Canada

**Background:** Electronic (e-) cigarettes are battery-powered devices that produce an aerosol by heating up a liquid composed of nicotine, flavouring agents, propylene glycol and vegetable glycerin (PGVG). In recent years, e-cigarettes have gained popularity among adolescents, raising concerns over the potential adverse effects in youth with respiratory diseases such as allergic asthma. In this study, we aimed to determine how a sub-chronic exposure to a flavoured aerosol affected airway and pulmonary inflammation in a murine model of allergic asthma.

**Methods:** Male and female C57BL/6 mice were exposed to a mint flavoured aerosol containing nicotine for 14 days. The control groups were exposed to air only or PGVG only. Then, three mice from each exposure group were euthanized immediately after the last aerosol exposure to characterize immediate effects of inhaled aerosols. The remaining mice from each group were sensitized and challenged with ovalbumin (OVA) to induce inflammation, a key feature of an asthmatic phenotype (Days 0, 7, 14-16), or treated with PBS as the control. We collected the serum, the bronchoalveolar lavage (BALF) and the lung tissue (Days 17, 19) to measure total serum IgE, characterize inflammation via flow cytometry, and measure gene transcription changes via RT-qPCR.

**Results:** Immunophenotyping of BALF immune cells revealed infiltration of eosinophils in the BALF of OVA-treated mice; in contrast, there were no eosinophils in the BALF of PBS-treated mice. Similarly, among air-exposed mice, the frequency of eosinophils in the lung tissue was significantly higher in OVA-treated mice compared to air-exposed mice treated with PBS. However, there was no difference in eosinophils frequency among PGVG- and JUUL-exposed mice treated with OVA or PBS. There were also no differences in the frequency of T cells in the lung tissue between any of the exposure groups. Overall, serum IgE was higher in OVA-treated mice compared to the respective PBS control group, but there was no difference between air- and JUUL-exposed mice.

**Conclusions:** This study is the first to investigate how a prior exposure to e-cigarette aerosols impacts the pulmonary inflammatory response in a murine model of allergic asthma. Overall, these results indicate that a past exposure to e-cigarettes did not significantly alter the immune cell composition of the BALF and lung tissue, and did not significantly exacerbate the humoral response in an ovalbumin-induced model of allergic asthma. Future studies should thus focus on the effects of a concurrent e-cigarette aerosol exposure in murine models of asthma.

## Day 1, Poster 29 - *Pseudomonas aeruginosa* evasion of neutrophil-mediated clearance in persistent Cystic Fibrosis infections

Sophia Goldman<sup>1,2</sup>, Kelly Kwong<sup>1,2</sup>, Annie Beauchamp<sup>2</sup>, Antonio DiGiandomenico<sup>3</sup>, Valerie Waters<sup>4</sup>, Dao Nguyen<sup>1,2,5</sup>

<sup>1</sup>Department of Microbiology & Immunology, McGill University, QC, Canada, <sup>2</sup>Meakins-Christie Laboratories, Research Institute of the McGill University Health Centre, QC, Canada, <sup>3</sup>Microbial Sciences, AstraZeneca, Gaithersburg, MD, USA, <sup>4</sup>Department of Laboratory Medicine and Pathobiology, University of Toronto, QC, Canada, <sup>5</sup>Department of Medicine, McGill University, QC, Canada

Chronic *Pseudomonas aeruginosa* (PA) infections in Cystic Fibrosis (CF) patients are associated with poor clinical outcomes such as a more rapid decline in lung function, respiratory failure, and premature death. New-onset PA infections are routinely treated with antibiotics such as inhaled tobramycin (TOB) to prevent the establishment of a chronic infection. Unfortunately, eradication therapy often fails in up to 40% of patients due to reasons that are poorly understood leaving patients to develop a persistent PA infection. The Nguyen lab recently showed that PA isolates from CF patients who failed eradication therapy were more resistant to neutrophil-mediated opsonophagocytosis and intracellular bacterial killing (OPK) and lacked twitching motility compared to isolates from eradicated infections. Novel alternative treatments such as MEDI3902, a new bispecific monoclonal antibody targeting the exopolysaccharide Psl and the type III secretion system protein PcrV to enhance neutrophil-mediated OPK, are needed to improve the eradication of new-onset PA infections. Clinical PA isolates were collected from a cohort study of CF children (aged 0-18 years old) at the Hospital for Sick Children, Toronto, Canada. Sputum samples were collected from CF children with a new-onset PA infection prior to treatment with TOB. A murine pulmonary infection model was used to determine the effect of MEDI3902 treatment regimens on bacterial clearance in persistent PA isolates. We performed an in vivo mixed infection to determine if restoration of pilus-mediated twitching motility in a persistent PA isolate will increase its susceptibility to neutrophil phagocytosis and reduce the pulmonary bacterial burden. Using these results, competitive index values were generated to assess the fitness of each strain in vivo. Our results show restoration of pilus-mediated twitching motility in a non-twitching persistent PA isolate significantly improved in vivo bacterial clearance generating CI values below 1.0. Preliminary studies suggest that a prophylactic dose of MEDI3902 reduces in vivo bacterial burden, with the greatest effect occurring when a booster dose at 24h post-infection is given.

## **Day 1, Poster 15 - Mitochondrial fission contributes to diaphragmatic weakness induced by mechanical ventilation**

Haikel Dridi<sup>1</sup>, Mohamad Yehya<sup>2</sup>, Robert Barsotti<sup>3</sup>, Yang Liu<sup>1</sup>, Steve Reiken<sup>1</sup>, Lan Azria<sup>2</sup>, Qi Yuan<sup>1</sup>, Rajesh Kumar Soni<sup>4</sup>, Andrew Marks<sup>1</sup>, Alain Lacampagne<sup>2</sup>, Stephan Matecki<sup>2</sup>

<sup>1</sup> Columbia University Vagelos College of Physicians and Surgeons, <sup>2</sup>montpellier university, <sup>3</sup>Philadelphia College of Osteopathic Medicine Philadelphia, <sup>4</sup>Herbert Irving Comprehensive Cancer Center, New York,

In critical care patients, acute diaphragm unloading due to mechanical ventilation (MV) initiates a process of diaphragmatic dysfunction and atrophy referred to as ventilator-induced diaphragm dysfunction (VIDD). Although, mitochondrial dysfunction linked to oxidative stress, plays a critical role in VIDD, the precise molecular mechanism remains poorly understood. Herein, we show, that six hours of MV resulted in a mitochondrial fission process with reduction of mitochondria size and interaction associated with increase dynamin related protein 1 (DRP1) expression that all are prevented by P110, a molecule that blocks the recruitment of DRP1 to the mitochondrial membrane. Moreover, isolated mitochondria from MV diaphragms exhibited decreased oxygen consumption and an increase of ROS production. These mitochondrial alterations were associated with a rapid oxidation of ryanodine receptor type 1 as well as depletion of the stabilizing subunit calstabin 1. Subsequently, we observed that the sarcoplasmic reticulum (SR) from the MV diaphragms was leaky to Ca<sup>2+</sup> and associated with reduced diaphragmatic contractile function. All these changes were prevented by the mitochondrial fission inhibitor molecule P110.

Taken together, the results from our study show that MV induces mitochondrial fragmentation and dysfunction in the diaphragms that is associated with an up/down regulation of 320 proteins, mainly related to mitochondrial function. These results emphasize the importance of molecules targeting mitochondrial fission/fusion balance such as P110 to prevent VIDD in human.

# Day 1, Poster 9 - The effect of obstructive sleep apnea on cognitive functioning among Parkinson's disease individuals: Evidence from the Canadian Longitudinal Study on Aging (CLSA).

Teresa Gomes<sup>1, 2</sup>, Andrea Benedetti<sup>2, 3</sup>, Anne-Louise Lafontaine<sup>4</sup>, Nadia Gosselin<sup>5</sup>, Ron Postuma<sup>6</sup>, Richard John Kimoff<sup>2, 7</sup>, Marta Kaminska<sup>2, 7</sup>

<sup>1</sup>Department of Integrated Program in Neuroscience, McGill University, Montreal, Quebec, Canada ,

<sup>2</sup>Translational Research in Respiratory Diseases, Research Institute of the McGill University Health Centre, Montreal, Quebec, Canada , <sup>3</sup>Department of Medicine and Department of Epidemiology, Biostatistics & Occupational Health, McGill University Health Centre, Montreal, Quebec, Canada ,

<sup>4</sup>Montreal Neurological Hospital, McGill University Centre, Montreal, Quebec, Canada, <sup>5</sup>Research Center, CIUSSS

Nord-de-l'Ile-de-Montreal, Montreal, Quebec, Canada, <sup>6</sup>Department of Neurology and Neurosurgery, McGill University, Montreal General Hospital, Montreal, Quebec, Canada, <sup>7</sup>Respiratory Division and Sleep Laboratory, McGill University Health Centre, Montreal, Quebec, Canada

**Introduction and aim:** Obstructive sleep apnea (OSA) is associated with cognitive decline in the general older population and with lower cognition in Parkinson's disease (PD) patients in clinical cohorts. We aimed to evaluate associations between high risk for OSA and cognition in individuals with (PD) from a population cohort.

**Methods:** Participants with PD were identified in Canadian Longitudinal Study of Aging (CLSA) comprehensive cohort at baseline or at 3-year follow-up using a validated algorithm. High risk of OSA was determined using the STOP (Loud **S**nooring, **T**iredness/**S**leepiness, **O**bserved apneas and high blood **P**ressure)  $\geq 2$  . Cognitive measures included: the Rey Auditory Verbal Learning Test (RAVLT) - immediate and 5-min delayed recall; Animal Fluency Test (AFT), the Mental Alternation Test (MAT); Controlled Oral Word Association Test (COWAT), Stroop Test- Victoria Version, Prospective Memory Test (PMT and TMT), and Choice reaction times (CRT) task. Linear regression was performed to assess relationships between STOP and cognitive measures, adjusted for potential cofounders.

**Results:** We identified 89 individuals at baseline and 61 additional patients at the 3-yr follow-up. Overall, 55 had a high risk of OSA (mean age 70.9 (8.8) years, 72.7% male) and 95 did not (mean age 69.5 (9.2) years, 63.2% male). There was significant association between OSA risk and cognitive measures MAT ( $p=0.02$ ) and COWAT ( $p=0.03$ ) in adjusted analyses.

**Conclusion:** High risk of OSA was associated with poorer results on executive function tests in PD participants. Longitudinal assessment within the CLSA may provide additional insights into the potential impact of OSA on the evolution of cognitive function in PD.

**Acknowledgments:** CLSA National Coordinating Centre; funding: CSCN, CIHR.

# Day 2 Oral - Intermittent Glucocorticoid Therapy Prevents Signs of Trained Innate Immunity in Macrophages from Muscular Dystrophy (mdx) Mice

Tom Podolsky<sup>1,2</sup>, Feng Liang<sup>1,2</sup>, Ekaterina Gusev<sup>1,2</sup>, Qian Li<sup>1,2</sup>, Basil J Petrof<sup>1,2</sup>

<sup>1</sup>Meakins-Christie Laboratories, Translational Research in Respiratory Diseases Program, Reserach Institute of the McGill University Health Centre, <sup>2</sup>Respiratory Division, Department of Medicine, McGill University Health Centre

**Background:** Duchenne Muscular Dystrophy (DMD) is a genetic disease caused by lack of the protein dystrophin, leading to chronic muscle fiber damage. In addition to the primary genetic defect, secondary inflammation is a significant driver of disease pathogenesis. Dysregulated macrophage (MP) function has been directly implicated in both necrosis and fibrosis of DMD muscles. In the mdx mouse model of DMD, we recently reported evidence for trained immunity in bone marrow-derived macrophages (BMDM) even prior to their entry into dystrophic muscles (*Bhattarai et al, Nature Communications 2022*). Trained immunity occurs when a primary insult, such as exposure to microbial components or tissue damage molecules, “trains” the innate immune system to be hyperresponsive to later secondary insults via epigenetic reprogramming of the cells. We have proposed that systemic exposure to molecules released from dystrophic muscles induces trained immunity at the bone marrow level in DMD. Clinically, DMD patients are treated with glucocorticoids (GCs), but the ability of this treatment to modulate trained immunity is unknown. The purpose of this study was to determine if either daily or intermittent GC treatment can prevent the transcriptional hyperresponsiveness of mdx BMDM to heterologous stimuli, which is a hallmark feature of trained immunity. In addition, we investigated whether this is associated with changes in either MP infiltration or contractile function of the dystrophic diaphragm muscle.

**Hypothesis:** We hypothesized that GCs could exert their beneficial effects via inhibition of trained immunity, and that the impact of GC treatment on this response would differ between daily (5 days per week) and intermittent (once-a-week) dosing.

**Methods:** Male mdx mice (5 wks old, n=12 per group) were treated for 1 month with either daily or intermittent GC (prednisolone) or PBS (sham treatment). At the end of the treatment period, BMDM were cultured for a week (“rest period”) without any exposure to GCs. The cells were then separately exposed to 4 distinct heterologous stimuli (LPS+IFN- $\gamma$ , IL-4, Fibrinogen,  $\beta$ -Glucan), and qPCR was performed to measure transcriptional responses of typical pro-inflammatory M1 (TNF- $\alpha$ , iNOS, IL-6, IL-12 $\alpha$ ) and anti-inflammatory M2 (Arg1, YM1, CD206, TGF- $\beta$ ) genes. In the diaphragm, flow cytometry quantified intramuscular MPs and contractility was measured by *ex vivo* electrical stimulation.

**Results:** For pro-inflammatory M1 genes, both daily and intermittent GC treatment for 1 month greatly reduced the transcriptional responsiveness of mdx BMDM to the different forms of stimulation. In contrast, for anti-inflammatory M2 genes only the daily GC regimen reduced transcriptional responsiveness of mdx BMDM. This general pattern was consistent across the heterologous stimuli for all of the M1 and M2 genes evaluated. In addition, intermittent GC treatment resulted in a significant reduction of diaphragm MPs as well as increased force-generating capacity of the diaphragm.

**Conclusions:** In macrophages obtained directly from the bone marrow of dystrophic mice, daily GC therapy *in vivo* had broad inhibitory effects on both M1 and M2 gene responsiveness, whereas intermittent GC treatment (once-a-week) only inhibited pro-inflammatory M1 gene responses. Intermittent GC therapy was also associated with reduced diaphragm inflammation and improved contractile function. These findings suggest that once-a-week GC therapy may be effective and help to avoid the known side effects of daily therapy. Further work is needed to determine whether daily and intermittent GCs have differential effects on the epigenetic reprogramming associated with trained immunity.



## Day 2, Poster 17 - The Effects of E-cigarette Use on Cardiopulmonary Health

Vincenza Caruana<sup>1,2</sup>, Koren Mann<sup>1,3</sup>, Carolyn Baglole<sup>1,2,4,5</sup>

<sup>1</sup>Department of Pharmacology and Therapeutics, McGill University, Montreal, QC, Canada, <sup>2</sup>Meakins-Christie Laboratories, McGill University, <sup>3</sup>Lady Davis Institute for Medical Research, Montreal, QC, Canada, <sup>4</sup>Research Institute of the McGill University Health Centre, Montreal, QC, Canada, <sup>5</sup>Department of Medicine, McGill University, Montreal, QC, Canada

E-cigarettes were designed to simulate the act of cigarette smoking without the injurious health effects of tobacco. Although e-cigarettes were intended to be a cessation tool for smokers, their sleek design and flavorings made them popular among teens and young adults. Yet, the health effects of e-cigarette use in non-smokers remains unclear. Several studies have correlated e-cigarette aerosols to increased inflammation and pathological conditions such as myocardial infarctions and organ fibrosis. Therefore, this project investigates the impact of a chronic, high-level e-cigarette exposure on multiple pulmonary and cardiovascular outcomes, including fibrosis and atherosclerosis. To model atherosclerosis, 5-week-old male and female C57BL/6J mice were injected with AAV-PCSK9 and fed a high fat diet. One week later, the mice were exposed to room air or the e-cigarette aerosol twice daily for 16 weeks. The commercially available e-cigarette brands STLTH and Vuse were used as they are among the most popular e-cigarette brands used today. After the exposure period, metal deposition, inflammatory and fibrotic markers in the lungs will be assessed. The extent of the atherosclerotic plaque and its constituents will be evaluated by *en face* oil red O staining, picrosirius red,  $\alpha$ -smooth muscle actin, and MOMA-2 staining. These results have the potential to make significant impacts in understanding the long-term health consequences of vaping.

## Day 2, Poster 30 - Characterization of a novel casein-specific anaphylactic mouse model

Wei Zhao<sup>1,2</sup>, Eisha Ahmed<sup>1</sup>, Nicholas Vonniessen<sup>1,2</sup>, Casey Cohen<sup>1,2</sup>, Bruce Mazer<sup>1,2</sup>

<sup>1</sup>The Research Institute of the McGill University Health Centre and the Department of Pediatrics, Faculty of Medicine, McGill University, Montreal, Canada, <sup>2</sup>Meakins-Christie Laboratories, McGill University

**Rationale:** Cow's milk allergy, caused by ingestion of proteins such as casein, is one of the leading causes of anaphylaxis in children. Mouse models that mimic anaphylaxis in humans are needed to evaluate potential new therapies for food allergy. Since severe eczema is associated with food allergy in children and may be the portal of sensitization, we established a mouse model in which the mice are transdermally sensitized.

**Methods:** Six- to eight-week-old male and female C57BL/6 mice (n=3-5) were exposed via gently abraded skin to dissolved casein or PBS weekly for six weeks. Two weeks after the last sensitization, all mice were challenged intragastrically with 15mg of dissolved milk powder. The challenged mice were placed in an observation chamber with live and infrared cameras to assess clinical symptoms and skin surface temperature. Following sacrifice, tissue samples including spleen, mesenteric lymph nodes, Peyer's patches, inguinal lymph nodes, and axillary lymph nodes were assessed.

**Results:** Following casein sensitization, we detected casein-specific IgE in all sensitized female mice which peaked on day 28. IgE+ B cells were significantly increased in the inguinal lymph nodes of sensitized female mice compared to controls. We also observed moderate anaphylactic reactions including continuous scratching and decreased reactivity from the female casein-sensitized mice.

**Conclusion:** These findings suggest that four weekly transdermal sensitizations were sufficient to induce systemic reactions in intragastrically challenged female C57BL/6 mice. This mouse model can serve as a preclinical model to determine the efficacy of potential treatments for food allergy.

# Day 1, Poster 20 - Synergistic Implications of IL-17A in the Modulation of Neutrophilic Airway Inflammation by Bronchial Epithelial Cells

Wided Akik<sup>1,2</sup>, Nurlan Dauletbaev<sup>3,4</sup>, Larry C. Lands<sup>2,3</sup>

<sup>1</sup>Division of Experimental Medicine, Faculty of Medicine and Health Sciences, McGill University, Montreal, Quebec, Canada, <sup>2</sup>Meakins-Christie Laboratories, Research Institute of the McGill University Health Centre, Montreal, Quebec, Canada, <sup>3</sup>Department of Pediatrics, Faculty of Medicine and Health Sciences, McGill University, Montreal, Quebec, Canada, <sup>4</sup>Department of Internal, Respiratory and Critical Care Medicine, Faculty of Medicine, Philipps-University of Marburg, Marburg, Germany

**Background:** Chronic neutrophilic lung diseases, such as severe neutrophilic asthma are characterized by increased airway IL-17A and neutrophilia. IL-17A enhances recruitment of neutrophils by inducing epithelial production of IL-8, the primary chemoattractant for neutrophils into the airway. IL-17A also has the ability to cooperate with other pro-inflammatory cytokines, mainly TNF- $\alpha$ , to enhance inflammatory cell response. The exact mechanisms by which IL-17A and TNF- $\alpha$  drives the development of neutrophilic airway inflammation are as yet unclear. We propose that understanding the transcriptional role of the combination of IL-17A and TNF- $\alpha$  in neutrophilic lung inflammation will lead to new targeted therapies. The combinatorial effects of IL-17A and TNF- $\alpha$  on the modulation of IL-8 and other neutrophil-mobilizing mediators in human bronchial epithelial cells were investigated.

**Methods:** Human bronchial epithelial cells (BEAS-2B and NHBE) were exposed to IL-17A and TNF- $\alpha$  as a single stimulus or co-stimulated (10 - 100 ng/mL). The release (ELISA) and the kinetics of mRNA expression (qPCR) of IL-8, G-CSF, and MCP-1 in response to IL-17A and TNF- $\alpha$  were examined. NF- $\kappa$ B transactivation (luciferase reporter assay, p65 phosphorylation, p65 nuclear activation) was also assessed. Inflammatory responses were evaluated by computational approaches (multidimensional scaling). The degree of synergy was quantified using the Highest Single Agent (HSA) model.

**Results:** IL-17A and TNF- $\alpha$  each upregulated IL-8, G-CSF, and MCP-1 production in a dose- and time-dependent manner. The combination of IL-17A and TNF- $\alpha$  synergistically amplified IL-8 and G-CSF release and expression, with no synergistic effect seen for MCP-1. The dual stimuli synergistically increased NF- $\kappa$ B-dependent luciferase activity, but there was no synergistic increase in p65 transactivation levels. Different magnitudes and patterns of synergistic upregulation of analytes by the combination of IL-17A and TNF- $\alpha$  support that the synergistic effects cannot be simply explained by NF- $\kappa$ B transactivation and may involve the interplay of upstream regulators and downstream effectors linked to NF- $\kappa$ B. Other transcriptional signaling mechanisms may include the participation of other transcription factors or enhanced p65 occupancy on promoters or increased chromatin accessibility leading to airway hyperinflammation.

**Conclusions:** The combination of IL-17A and TNF- $\alpha$  synergistically induced a hyperinflammatory cell response that is in part mediated by NF- $\kappa$ B transactivation. Next experiments will examine IL-8, G-CSF, and MCP-1 gene regulation by comparing 5' and 3' untranslated regions (UTR) sequences and structures using computational system approaches. To further explore the interactions of IL-17A and TNF- $\alpha$  *in vivo*, a murine model of house dust mite (HDM)-induced airway inflammation will be used. This will give more insights into the impact of the combination of IL-17A and TNF- $\alpha$  on neutrophilic inflammation.

## Day 2, Poster 23 - The Aryl Hydrocarbon: New Implications in Fibrosis

Willem Rijnbout-St.James<sup>1, 2, 3</sup>, Jun Ding<sup>1, 4, 5</sup>, David Eidelman<sup>1, 4</sup>, Celeste Laporte<sup>3</sup>, Carolyn Baglole<sup>1, 2, 3, 4</sup>

<sup>1</sup>Meakins-Christie Laboratories, <sup>2</sup>Translational Research in Respiratory Diseases Program at the Research Institute of the McGill University Health Centre, <sup>3</sup>Department of Pathology, <sup>4</sup>Department of Medicine, <sup>5</sup>Division of Experimental Medicine

**Background:** Interstitial lung diseases (ILD) are a family of lung pathologies characterized by diffuse inflammation and fibrosis. The most common ILD is idiopathic pulmonary fibrosis (IPF), for which patients have a median survival of 3 years from diagnosis<sup>1</sup>. There is no cure for IPF, highlighting the need to better understand the molecular mechanisms driving the fibrotic response to develop effective therapeutic approaches. Dysregulated signaling activates lung fibroblasts, key effector cells in fibrosis, resulting in overproduction of the extracellular matrix (ECM) proteins that stiffens the lungs. One pathway may involve the aryl hydrocarbon receptor (AhR), a ubiquitously expressed transcription factor which regulates expression of genes typically involved in drug metabolism, such as cytochrome P450 enzymes, by binding to its cognate response element called the DRE; the AhR also increases ECM genes. While this canonical AhR signaling pathway has been well characterized, AhR non-canonical signaling is poorly understood. Our preliminary data shows that, in response to the profibrotic cytokine transforming growth factor beta (TGF- $\beta$ ), the AhR drives collagen production, a key component of the ECM; however, the extent to which AhR controls mechanisms of fibrosis is completely unknown.

**Hypothesis:** AhR regulates fibrosis by modulating molecular signaling pathways that contribute to collagen deposition via a non-canonical signaling pathway.

**Models and Experimental Design:** To investigate the contribution of a non-canonical AhR pathway to the development of fibrosis *in vitro*, lung fibroblasts were isolated from our established AhR-mutant mice; this includes AhR-wildtype (AhR-WT) and -knockout (AhR-KO) mice, as well as two AhR mutant mouse strains, AhR-NLS and AhR-DBD. The AhR-NLS strain contains an AhR that is incapable of translocating to the nucleus, while the AhR-DBD strain contains an AhR that cannot bind to DNA via its cognate response element, the DRE<sup>2</sup>. Mouse lung fibroblasts (MLFs) from AhR-WT and AhR-KO mice were treated with TGF- $\beta$  (5 ng/ml) for 24 and 48 hours and protein levels of COL1A1 and  $\alpha$ -smooth muscle actin ( $\alpha$ -SMA), a marker of myofibroblast differentiation, were evaluated using western blot to verify AhR-dependent collagen production.

**Results:** There was more COL1A1 protein in AhR-WT lung fibroblasts compared to AhR-KO lung fibroblasts even without TGF- $\beta$  exposure. In response to TGF- $\beta$ , COL1A1 and  $\alpha$ -SMA protein expression was not significantly increased.

**Future Directions:** I will confirm AhR-dependent collagen synthesis in response to TGF- $\beta$  by western blot and extend my investigation by using AhR-NLS and AhR-DBD MLFs in subsequent experiments. I will further analyze AhR-dependent changes in gene expression through RNA-sequencing (RNA-seq) and assess global protein expression using shotgun proteomics. I will also evaluate TGF- $\beta$ -induced AhR-dependent phosphorylation in MLFs using phosphoproteomics to collectively assess for novel pathways regulated by AhR that drive fibroblast function in response to profibrotic stimuli (e.g., TGF- $\beta$ ).

**Significance:** The poor survival rate of IPF underscores the need for a better understanding of IPF pathogenesis. This project will contribute new insights into the AhR-dependent mechanisms involved in fibrosis and may highlight previously unknown factors as therapeutic targets.

# **Day 1, Poster 27 - Leveraging multi-omics sequencing data to identify clinically relevant cell groups and the risk-associated biomarkers**

Yasmin Jolasun<sup>1,2</sup>, Jun Ding<sup>1,2</sup>

<sup>1</sup>Meakins-Christie Laboratories, McGill University, <sup>2</sup>Translational Research in Respiratory Diseases, Research Institute of the McGill University Health Centre

**Abstract:** Identifying new therapeutic drug targets is a crucial aspect of drug development research. Machine learning and deep learning approaches have been successfully used to address the challenge of biomarker discovery from various types of biological data sets. In this study, we focused on multi-omics sequencing data, such as single-cell sequencing and bulk RNAseq data.

However, the high cost of single-cell experiments, and the loss of cell and gene heterogeneity within a sample in bulk RNAseq experiments, pose challenges in identifying drug therapy targets for complex diseases. To overcome these difficulties, we propose a deep-learning model that leverages the abundant bulk RNAseq data with clinical information and high-resolution single-cell RNAseq data.

Our approach involves building a supervised deep-learning Cox regression model trained on bulk RNAseq data to predict disease outcomes in patients, along with a Variational Autoencoder with a modified loss function to identify high and low-risk cell populations and their associated biomarkers from single-cell data. These two modules will feed information iteratively to each other, guiding the identification of low and high-risk cells in each cell population and biomarkers associated with the disease risks.

Our proposed deep-learning model aims to identify clinically relevant cells and biomarkers that signify high-risk or low-risk cell populations captured by single-cell data, potentially leading to the development of novel diagnostic panels and therapeutic drug targets.

# Day 1, Poster 25 - Repurposing Drugs for IPF with Deep Generative Model and Single-nucleic RNA-seq Data

Yumin Zheng<sup>1,2</sup>, Jun Ding<sup>2,3</sup>

<sup>1</sup>Quantitative Life Sciences, McGill University, <sup>2</sup>Meakins-Christie Laboratories, <sup>3</sup>Division of Experimental Medicine, McGill

**Rationale:** Understanding the changes in cellular states of different cell populations (cell type or sub-types) across disease progression in the IPF lung tissue are crucial in understanding the regulation of disease and facilitating therapeutic target discoveries. However, the cellular dynamics across IPF progression remains poorly studied. Here, we develop a probabilistic graphical model that reconstructs the cellular dynamics for each cell population along IPF progression and repurposes drugs for IPF treatment.

**Methods:** We analyzed data of 89,377 nuclei obtained from the differentially affected region in IPF lungs, classified as IPF1, 2, and 3 based on tissue involvement as previously described by us (ref <https://doi.org/10.1172/jci.insight.131597>) as well as healthy controls. Gaussian density estimator is employed to cluster all the cells into 4 different IPF stages IPF0-IPF3 with varying extents of fibrosis based on the quantified alveolar surface density. Next, we built the cellular dynamics graph composed of nodes and edges with the proposed method UNAGI. A node in the graph represents a specific cell population while an edge shows the cell population changes across IPF stages. We employed a graph convolution neural network to concatenate the neighborhood information and, a beta variational autoencoder (beta-VAE) to learn the probability (density) distribution in the reduced latent space for the expression of all cells in each node. A node will be connected to its parent node in the preceding stage with an edge, where the parent node is defined as the node with a minimal KL divergence. The cellular dynamics for each cell population will be represented by a track in the graph (a set of edges that span from IPF0 to IPF3). For each track, the iDREM model was employed to reconstruct the underlying gene regulatory networks, which were feedback to refine the dynamics graph. The final dynamics graph was obtained by iterating between building the graph and learning the regulatory networks until convergence. Then we will use perturb the single cells by regulating the expression of genes according to Connectivity Maps drug profiles and use UNAGI to predict the perturbed latent space and measure the effectiveness of the potential drugs.

**Results:** A cellular dynamics graph was obtained, which represents the cellular dynamics for each cell population along IPF progression as tracks in the graph. For each track, we also obtained the regulatory networks and perturbation results for drug repurposing for IPF. The cellular dynamics graph (nodes, edges, tracks), the regulatory networks, and the perturbation results are all publicly available (and could be interactively interrogated) at <http://dinglab.rimuhc.ca/unagi>. **Conclusion:** The built probabilistic graph that describes the cellular dynamics and underlying regulatory networks presents an unprecedented opportunity to derive a deeper understanding of the role of each cell population in driving IPF disease progression, the perturbation module can computationally identify potential therapeutic targets and repurposed drugs. **Funding:** JCS: Department of Defense (W81XWH-19-1-0131), NK: NIH U01HL145567 and Three Lakes Foundation, JD: FRQS Junior 1 award (295298, 295299)